Radiation Model for Row Crops: I. Geometric View Factors and Parameter Optimization

P. D. Colaizzi,* S. R. Evett, T. A. Howell, F. Li, W. P. Kustas, and M. C. Anderson

ABSTRACT

Row crops with partial cover result in different radiation partitioning to the soil and canopy compared with full cover; however, methods to account for partial cover have not been adequately investigated. The objectives of this study were to: (i) develop geometric view factors to account for the spatial distribution of row crop vegetation; (ii) combine view factors with a widely used vegetation radiation balance model; and (iii) optimize three parameters required by the model that describe leaf angle, visible leaf absorption, and near-infrared leaf absorption. Measurements of transmitted and reflected shortwave irradiance for corn (*Zea mays* L.), grain sorghum [*Sorghum bicolor* (L.) Moench], and cotton (*Gossypium hirsutum* L.) were used to optimize parameters and evaluate the model. View factors were derived by modeling the crop rows as elliptical hedgerows. The optimized ellipsoid leaf angle parameter, visible leaf absorption, and near-infrared leaf absorption were 1.0, 0.85, and 0.20 for corn; 1.5, 0.82, and 0.20 for grain sorghum; and 3.0, 0.83, and 0.14 for cotton, respectively. Visible leaf absorption was similar for all crops. Near-infrared leaf absorption was the same for corn and grain sorghum but less for cotton. The only parameter that changed for each crop species was leaf angle. The optimized parameters for corn and grain sorghum were within the range of values recommended in previous studies, and the leaf angle parameter for cotton agreed with a previous study of cotton leaf angles. All parameters were distinctly identifiable, and no parameter correlation was observed.

Radiation is the primary driver of the energy and water balance of the soil–plant–atmosphere continuum. Models that describe the radiation environment of vegetation and soil have numerous applications in agriculture, hydrology, and meteorology. Examples of agricultural applications include models to calculate plant photosynthesis, net primary production, evapotranspiration (ET), gas exchange, and pest and disease vectors, which all require estimates of radiation partitioning between the soil and vegetation components. Models designed for agriculture have used various approaches to deal with at least three distinct, but interrelated, issues, including (i) the dependency of shortwave radiative transfer as a function of wavelength (i.e., green vegetation absorbs a greater portion of visible or photosynthetically active radiation [PAR] in the 400–700-nm spectrum than near-infrared radiation [NIR] in the 700–3000-nm spectrum); (ii) radiation extinction and scattering within the canopy (i.e., usually described by a leaf angle distribution function [LADF]); and (iii) the spatial distribution of the vegetation (often accounted for using view factors).

P.D. Colaizzi, S.R. Evett, and T.A. Howell, USDA-ARS, Conservation and Production Research Lab., P.O. Drawer 10, Bushland, TX 79012-0010; F. Li, Geoscience Australia, National Earth Observation Group, Cnr Jerrabomberra Av & Hindmarsh Dr, Symonston, ACT 2609, GPO Box 378, Canberra ACT 2601, Australia; W.P. Kustas and M.C. Anderson, USDA-ARS, Hydrology and Remote Sensing Research Lab., Building 007, BARC-West, Beltsville MD 20705-2350.

Received 18 March 2011. *Corresponding author (paul.colaizzi@ars.usda.gov).

Published in Agron. J. 104:225–240 (2012)
Posted online 5 Jan 2012
doi:10.2134/agronj2011.0082

Campbell and Norman (1998) gave procedures to calculate shortwave canopy transmittance and reflectance, where PAR, NIR, direct-beam, and diffuse components are calculated separately. The procedures have been widely used in agricultural applications (described below); many details of these procedures were based on the earlier work of Goudriaan (1977, 1988) and Chen (1984). Each procedure can be used to calculate the various components of reflected and transmitted radiation or combined to calculate the total soil and canopy radiation budget. Briefly, the dependency of radiative transfer on wavelength is accounted for by a leaf absorption parameter for the PAR and NIR spectra (ζ_{PAR} and ζ_{NIR}, respectively), which may be species dependent (e.g., Gausman and Allen, 1973). Transfer of direct-beam radiation is calculated through an extinction coefficient, which is a function of the ellipsoid LADF (i.e., projected leaf angles resemble the surface of an ellipsoid). The dependence of the leaf angle distribution on species is accounted for by altering the shape of the ellipsoid through a single parameter (X_E) to be oblate (for more horizontal leaves), prolate (for more vertical leaves), or spherical (for a uniform distribution of leaf angles) (Campbell, 1986, 1990). A range of X_E values exists in the literature for various crops (Campbell, 1986; Campbell and Norman, 1998), which may require refinement to describe local canopy conditions (e.g., Doraiswamy et al., 2004; Flerchinger et al., 2009). The transfer of diffuse radiation is calculated by integrating direct-beam transmittance and reflectance over a hemisphere. The radiation budget can be calculated at various depths in the canopy and so could be used in multilayered approaches (e.g., Zhao and Qualls, 2005; Xiao et al., 2006; Flerchinger et al., 2009); the simplest approach treats the canopy as a single layer

Abbreviations: DIFF, diffuse radiation; DIR, direct beam radiation; ET, evapotranspiration; LADF, leaf angle distribution function; LAI, leaf area index; NIR, near-infrared radiation; PAR, photosynthetically active radiation; RPAR, reflected photosynthetically active radiation; TPAR, transmitted photosynthetically active radiation.

but still accounts for second-order reflection from the soil, which can be significant for sparse or incomplete canopies.

For sparse or incomplete canopies, radiative transfer models often use some form of a view factor (i.e., the fractions of soil, vegetation, or sky appearing in a line, directional, or hemispherical view to each other). Perhaps the two most widely used approaches for estimating view factors are assuming the canopy region as a two- or three-dimensional geometric shape (e.g., rectangular or elliptical hedgerows, ellipsoids, or cubes) or in terms of a one-dimensional, semiempirical clumping index. Studies that used geometric shapes usually considered only measurements of transmitted PAR or shortwave irradiance to validate their model (Charles-Edwards and Thorpe, 1976; Arkin et al., 1978; Mann et al., 1980; Norman and Welles, 1983; Annandale et al., 2004; Oyarzun et al., 2007), although Pieri (2010a,b) used measurements of net radiation near the soil surface. Also, these studies were conducted under a very limited set of conditions such as crop, canopy height (h_C) and width (w_C), or leaf area index (LAI), except for Annandale et al. (2004) and Oyarzun et al. (2007), where measurements were obtained for multiple tree species and a vineyard. The clumping index approach uses a semiempirical factor, usually multiplied by the LAI, to account for the increased interception of radiation by nonrandomly distributed (also described as clumped) vegetation compared with randomly distributed vegetation (Nilson, 1971). It has been used to characterize the nonrandomness of forest canopies (e.g., Chen, 1996; Kucharik et al., 1999) and has been adapted to row crops including cotton (Kustas and Norman, 1999) and corn and soybean [*Glycine max* (L.) Merr.] (Anderson et al., 2005). Both geometric and clumping index approaches appear robust in that they have been used successfully for a wide variety of vegetation. Geometric approaches, however, are more amenable to resolving the soil into sunlit and shaded components, which has been shown to be an important consideration in energy balance and ET studies (Ham and Kluitenberg, 1993; Annandale et al., 2004; Williams and Ayars, 2005; Pieri, 2010b).

Relatively few studies have evaluated radiative transfer models for row crop canopies where more than one type of radiation flux was measured. Also, usually only total net radiation was reported in studies that used the clumping index approach under sparse or varying vegetation cover. Flerchinger et al. (2009) simulated transmitted, reflected, and upwelling longwave radiation for wheat (*Triticum aestivum* L.), corn, and soybean using the multilayered Simultaneous Heat and Water (SHAW) model. Their SHAW version included a provision for the clumping index, but this was set to 1.0 because they limited their study to full or nearly full canopy cover. Xiao et al. (2006) evaluated the SHAW model to calculate reflected shortwave, incoming and outgoing longwave, and net radiation for a corn canopy, although their main focus was to evaluate and refine methods to calculate incoming longwave radiation.

The Campbell and Norman (1998) procedure has been used in conjunction with the clumping index for a wide range of vegetation cover and species in two-source energy balance models to estimate ET (Kustas and Norman, 1999; Anderson et al., 2005; Li et al., 2005; French et al., 2007), but usually only total net radiation was measured in these applications. In an earlier study, Lascano et al. (1987) estimated evaporation and ET for a sparse cotton crop using the ENWATBAL model, where radiation partitioning to the crop and soil were based on the Chen (1984) model. Pieri (2010a) pointed out that in two-source energy balance models, most attention has been given to validating the scalar flux calculation, with disproportionately little attention given to various radiation components and their partitioning to the soil and canopy. Given that the Campbell and Norman (1998) procedure contains several simplifications of earlier work (i.e., Goudriaan, 1977) but retains enough detail to be appropriate for a variety of applications, it would be useful to conduct an evaluation for different radiation fluxes and various row crops for a range of vegetation cover. Also, it appears that no studies have used this procedure in conjunction with view factors based on geometric shapes to describe the nonrandom distribution of vegetation or to compare these to the simpler clumping index approach.

The objectives of this research were to: (i) develop geometric view factors to describe the nonrandom spatial distribution of row crop vegetation, (ii) use these view factors in conjunction with the Campbell and Norman (1998) radiative transfer model to calculate transmitted and reflected PAR and shortwave radiation, and (iii) estimate X_E, ζ_{PAR}, and ζ_{NIR} using an optimization procedure for three row crops, including corn, grain sorghum, and cotton, and determine if these parameters are distinctly identifiable using the model described here. Although X_E values have been established for corn and grain sorghum, their suitability for incomplete canopy cover where view factors are used is not well established. Furthermore, it appears X_E has not been evaluated specifically for cotton, and ζ_{PAR}, and ζ_{NIR} may require crop-specific values (Gausman and Allen, 1973).

MODEL OVERVIEW

Radiative transfer models of vegetated surfaces are typically developed and validated based on irradiance measurements above, below, or at specified heights within a canopy, with upward or downward views or both. Radiometers have three basic view geometries, which are described here as line (e.g., light bars), directional (e.g., infrared thermometers), or hemispherical (e.g., dome). In this study, parameter optimization and subsequent model performance was evaluated by considering two cases of measured irradiance fluxes, including (i) transmitted PAR and shortwave irradiance measured by upward-looking line radiometers at the soil surface and (ii) reflected PAR and shortwave irradiance measured by downward-looking hemispherical radiometers just above the canopy. A model schematic (Fig. 1) provides an overview of each calculated irradiance flux; computational details are as follows.

Transmitted Shortwave Radiation, Upward Line or Planar View

Shortwave radiation transmitted through a canopy can be measured by an upward-looking line radiometer, usually deployed at the soil surface. Assuming that, in the direction parallel to the crop rows, vegetation is uniformly distributed, extending the line view along the rows is equivalent to a planar view. A line radiometer includes a line view for direct-beam irradiance and also a line-integrated hemispherical view for diffuse irradiance (i.e., a hemispherical view integrated from the crop row center to the interrow center); however, the terms *line view* or *planar view* are used here for brevity and also to maintain distinction from true hemispherical radiometers,

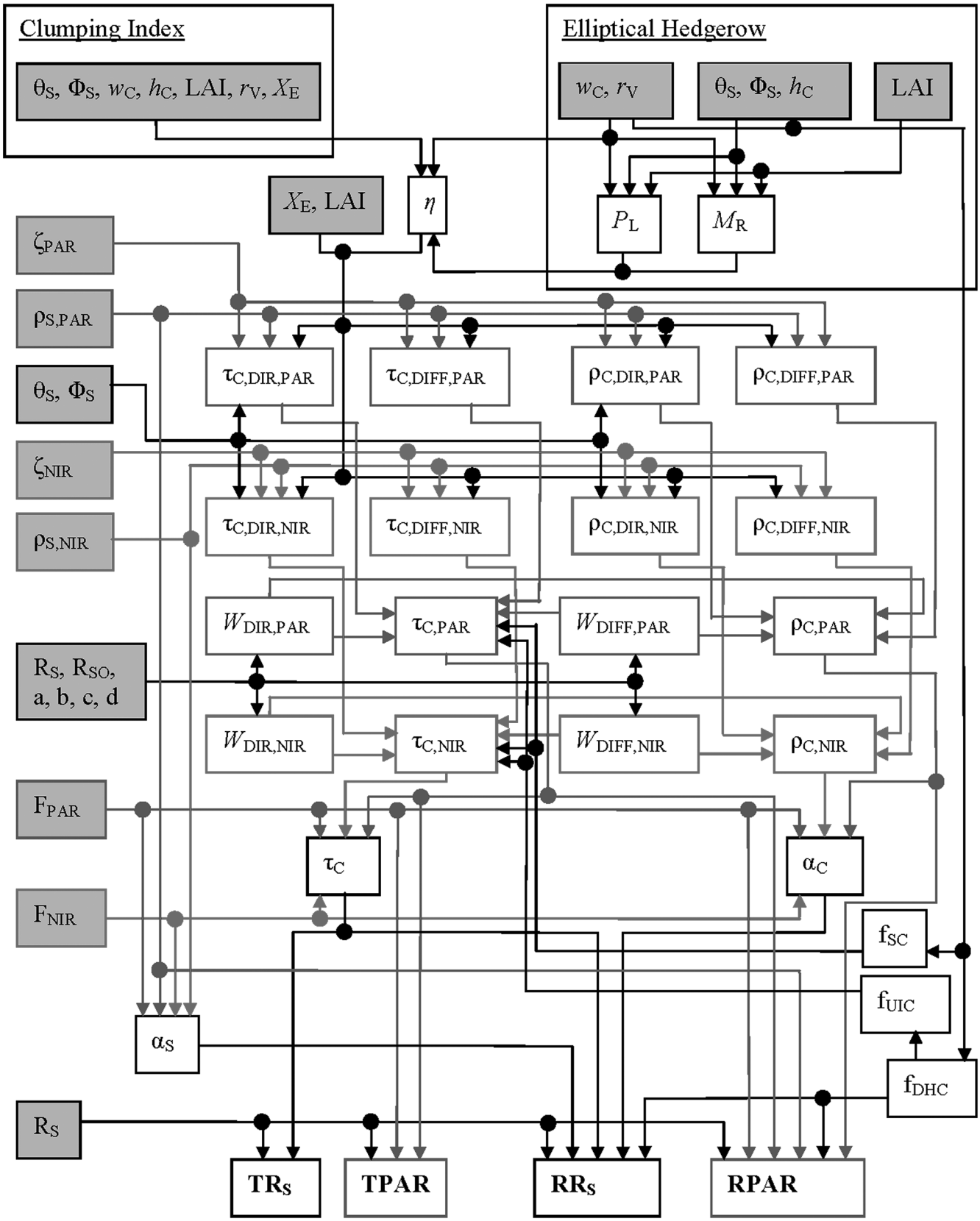

Fig. 1. Schematic of the Campbell and Norman (1998) model with the clumping index and elliptical hedgerow submodels. Gray boxes are model inputs and boxes with bold type are output fluxes used to optimize the ellipsoid leaf angle distribution function parameter (X_E), leaf absorption for photosynthetically active radiation (ζ_{PAR}), and leaf absorption for near-infrared radiation (ζ_{NIR}).

described below. Total transmitted shortwave irradiance to the soil surface (TR_S, W m^{-2}) was calculated as

$$TR_S = R_S \tau_C \quad [1]$$

where R_S (W m^{-2}) is global incoming shortwave irradiance, and τ_C is the fraction of shortwave radiation transmitted through the canopy. For a row crop with partial canopy cover, a portion of the transmitted radiation will reach the soil surface directly (unobstructed by the canopy), and the remainder will be transmitted through the canopy. This was accounted for in τ_C using two geometric view factors for beam and diffuse irradiance that were developed in this study. Furthermore, extinction through a canopy is dependent on the beam angle, meaning that transmittance will be different for the direct-beam and diffuse radiation components, where the latter is the transmittance for a direct beam integrated over all angles (Campbell and Norman, 1998). Shortwave transmittance also depends on the wavelength because vegetation absorbs a greater portion of PAR than NIR wavelengths. Therefore, τ_C is calculated by partitioning each component by weighing and view factors:

$$\begin{aligned}\tau_C = {} & F_{PAR}\left[W_{DIR,PAR}\left(f_{SC}\tau_{C,DIR,PAR}+1-f_{SC}\right)\right. \\ & \left. +W_{DIFF,PAR}\left(f_{UIC}\tau_{C,DIFF,PAR}+1-f_{UIC}\right)\right] \\ & +F_{NIR}\left[W_{DIR,NIR}\left(f_{SC}\tau_{C,DIR,NIR}+1-f_{SC}\right)\right. \\ & \left. +W_{DIFF,NIR}\left(f_{UIC}\tau_{C,DIFF,NIR}+1-f_{UIC}\right)\right]\end{aligned} \quad [2]$$

where F_{PAR} and F_{NIR} are the fractions of shortwave radiation in the PAR and NIR bands, respectively, $W_{DIR,PAR}$ and $W_{DIFF,PAR}$ are the weighing factors for direct beam (DIR) or diffuse (DIFF) radiation, respectively, in the PAR wavelengths, $W_{DIR,NIR}$ and $W_{DIFF,NIR}$ are the weighing factors for DIR and DIFF, respectively, in the NIR wavelengths, $\tau_{C,DIR,PAR}$ and $\tau_{C,DIFF,PAR}$ are the transmittance for DIR and DIFF, respectively, in the PAR wavelengths, $\tau_{C,DIR,NIR}$ and $\tau_{C,DIFF,NIR}$ are the transmittance for DIR and DIFF, respectively, in the NIR wavelengths, f_{SC} is the solar– canopy view factor (i.e., the fraction of canopy visible from the solar beam view angle), f_{UIC} is the upward-line-integrated hemispherical canopy view factor (i.e., the fraction of canopy visible when an upward-looking hemispherical view is integrated from the crop row center to the interrow center), and all terms in Eq. [2] are dimensionless. At our study location (Bushland, TX), F_{PAR} has been found to be nearly constant at 0.457 throughout the year (unpublished data, 1992), a result consistent with other locations in the western United States (McCree, 1972; Meek et al., 1984). The F_{NIR} is the unit complement of F_{PAR} (i.e., $F_{NIR} = 1.0 - F_{PAR}$). The weighing factors $W_{DIR,PAR}$ and $W_{DIR,NIR}$ were calculated in a manner similar to Weiss and Norman (1985), and $W_{DIFF,PAR}$ and $W_{DIFF,NIR}$ are the unit complements of $W_{DIR,PAR}$ and $W_{DIR,NIR}$, respectively (see Appendix 1 for calculation procedures). The f_{SC} and f_{UIC} terms were developed in this study as part of the geometric approach to account for the nonrandom spatial distribution of row crop vegetation, where rows were modeled as elliptical hedgerows, somewhat similar to Charles-Edwards and Thornley (1973) and Annandale et al. (2004). Procedures to calculate f_{SC} are given in Appendix 2; briefly, f_{SC} is a function of solar zenith and azimuth (relative to the crop row) angles, canopy height, canopy width, and row spacing but not canopy density, which is accounted for by τ_C. Procedures to calculate f_{UIC} are given in Appendix 3. In the clumping index approach, $f_{SC} = f_{UIC} = 1$, and a nonrandom spatial distribution of vegetation is accounted for through the $\tau_{C,DIR,PAR}$, $\tau_{C,DIFF,PAR}$, $\tau_{C,DIR,NIR}$, and $\tau_{C,DIFF,NIR}$ terms as described below.

Direct-beam PAR transmittance ($\tau_{C,DIR,PAR}$) was calculated following Campbell and Norman (1998) for a single-layer canopy as

$$\tau_{C,DIR,PAR} = \frac{\left(\rho_{C,PAR}{}^{*2}-1\right)\exp\left(-\sqrt{\zeta_{PAR}}K_{BE}\eta LAI\right)}{\left[\begin{array}{l}\left(\rho_{C,PAR}{}^{*}\rho_{S,PAR}-1\right)+ \\ \rho_{C,PAR}{}^{*}\left(\rho_{C,PAR}{}^{*}-\rho_{S,PAR}\right)\exp\left(-2\sqrt{\zeta_{PAR}}K_{BE}\eta LAI\right)\end{array}\right]} \quad [3]$$

where $\rho_{C,PAR}{}^{*}$ is the beam PAR reflection coefficient for a deep canopy with nonhorizontal leaves, ζ_{PAR} is the PAR absorption of leaves, K_{BE} is the extinction coefficient for direct-beam radiation, η is a factor used to account for the nonrandom spatial distribution of vegetation (i.e., row crops) and is described below, LAI is the leaf area index (m^2 m^{-2}), and $\rho_{S,PAR}$ is the PAR reflectance of the soil. The reflectance terms ($\rho_{C,PAR}{}^{*}$ and $\rho_{S,PAR}$) in Eq. [3] account for enhanced downwelling radiation that is reflected from the soil and re-reflected by canopy leaves. Goudriaan (1988) (cited in Campbell and Norman, 1998) calculated $\rho^{*}_{C,PAR}$ as

$$\rho_{C,PAR}{}^{*} = \frac{2K_{BE}\rho_{HOR,PAR}}{K_{BE}+1} \quad [4]$$

where $\rho_{HOR,PAR}$ is the beam reflection coefficient for a canopy with horizontal leaves, given as

$$\rho_{HOR,PAR} = \frac{1-\sqrt{\zeta_{PAR}}}{1+\sqrt{\zeta_{PAR}}} \quad [5]$$

Direct-beam NIR transmittance ($\tau_{C,DIR,NIR}$ in Eq. [2]) was calculated in the same manner as $\tau_{C,DIR,PAR}$ except that ζ_{PAR} was replaced with ζ_{NIR} (i.e., NIR absorption) in Eq. [3] and [5] (resulting in $\rho_{HOR,NIR}$ in Eq. [4] and [5] and $\rho_{C,NIR}{}^{*}$ in Eq. [3] and [4]), and $\rho_{S,PAR}$ was replaced with $\rho_{S,NIR}$ in Eq. [3]. Diffuse transmittance ($\tau_{C,DIFF,PAR}$ and $\tau_{C,DIFF,NIR}$ in Eq. [2]) was calculated by numerically integrating $\tau_{C,DIR,PAR}$ and $\tau_{C,DIR,NIR}$ over a half-sphere. Hence calculating transmittance in the different spectral bands (PAR and NIR) requires changing only two parameters (ζ_{PAR} vs. ζ_{NIR} and $\rho_{S,PAR}$ vs. $\rho_{S,NIR}$).

The canopy beam extinction (K_{BE}) was calculated based on the ellipsoidal LADF of Campbell (1990):

$$K_{BE} = \frac{\sqrt{X_E^2+\tan^2\theta_S}}{X_E+1.774\left(X_E+1.182\right)^{-0.733}} \quad [6]$$

where X_E is the ratio of horizontal to vertical projected unit area of leaves, and θ_S is the solar zenith angle. The X_E parameter quantifies the average leaf angle and is species specific; for the spherical, vertical, and horizontal leaf angle distributions, X_E = 1.0, 0, and ∞, respectively. The X_E, ζ_{PAR}, and ζ_{NIR} parameters were optimized for each crop based on maximizing an objective function as described below.

Soil reflectance ($\rho_{S,PAR}$ and $\rho_{S,NIR}$) were assumed to be 0.15 and 0.25, respectively, based on reflectance measurements over dry bare soil at the study location (Howell et al., 1993; Tunick et al., 1994), which is consistent with values suggested

by Campbell and Norman (1998). The respective $\rho_{S,PAR}$ and $\rho_{S,NIR}$ values were reduced to 0.09 and 0.15 for wet bare soil, also based on reflectance measurements at the study location and consistent with measurements reported by Graser and Van Bavel (1982) over a silty clay soil. The wet and dry reflectance values were varied linearly as a function of the water content in the top layer of soil during Stage 1 drying (i.e., the energy-limited stage; Idso et al., 1974) in a manner similar to Evett and Lascano (1993) for soil albedo. The maximum water content during Stage 1 drying was taken as 15 mm (NRCS, 2011). Following a wetting event, cumulative evaporation in the topsoil layer was calculated using the Penman–Monteith equation (Allen et al., 1998) until it reached 15 mm (or the total amount of the wetting event, if it was <15 mm). Additional soil water evaporation will occur during Stage 2 drying (e.g., Evett et al., 1995); however, it was assumed that the soil surface was dry at the end of Stage 1 drying (Idso et al., 1974), and $\rho_{S,PAR}$ and $\rho_{S,NIR}$ returned to 0.15 and 0.25, respectively.

The nonrandom spatial distribution of row crops was accounted for by multiplying the field LAI in the $\tau_{DIR,PAR}$ and $\tau_{DIR,NIR}$ formulations by a factor (η) that was calculated in two ways, either using a geometric approach where canopy rows were modeled as elliptical hedgerows (Charles-Edwards and Thornley, 1973; Annandale et al., 2004) or using the clumping index approach (Anderson et al., 2005). For the geometric approach,

$$\eta = \frac{r_V}{w_C} P_L M_R \quad [7]$$

where r_V is the crop row spacing (m), w_C is the canopy width (m), P_L is the path length fraction of a solar beam propagating through a canopy relative to nadir (dimensionless), and M_R is a multiple-row factor that accounts for a solar beam traversing across more than one canopy row (dimensionless); equations for P_L and M_R are given in Appendix 4. The r_V/w_C term in Eq. [7] converts the field LAI to a local LAI (i.e., within the canopy row). For the clumping index approach, $\eta = \Omega_{SW}/\cos(\theta_S)$, where Ω_{SW} is the clumping index calculated for shortwave extinction following Anderson et al. (2005). Briefly, Ω_{SW} is calculated using the same input parameters as the elliptical hedgerow approach (i.e., h_C, w_C, LAI, r_V, X_E, θ_S, and Φ_S), but simple empirical equations are used that have r_V–specific constants. In the clumping index approach, no view factors are explicitly used (i.e., $f_{SC} = f_{UIC} = 1$ in Eq. [2]); instead it is assumed that the impact of view factors can be implicitly accounted for in Ω_{SW} and hence η.

Transmitted PAR (TPAR) through a canopy is calculated in the same manner as TR_S, except only the PAR components are considered:

$$TPAR = R_S\left(4.602 F_{PAR}\right)\tau_{C,PAR} \quad [8]$$

where 4.602 converts radiation flux (W m^{-2}) to quantum flux (μmol m^{-2} s^{-1}; McCree, 1972), and

$$\tau_{C,PAR} = F_{PAR}\left[W_{DIR,PAR}\left(f_{SC}\tau_{C,DIR,PAR} + 1 - f_{SC}\right) + W_{DIFF,PAR}\left(f_{UIC}\tau_{C,DIFF,PAR} + 1 - f_{UIC}\right)\right] \quad [9]$$

Reflected Shortwave Radiation, Downward Hemispherical View

Shortwave radiation reflected from a vegetated surface can be measured by an inverted radiometer with a hemispherical view. For a row crop with partial canopy cover, some of the radiation will be reflected directly from the soil surface, with the remainder being reflected from the canopy. Because canopies are porous, some radiation reflected by the canopy will include both vegetation and soil components, where the latter is not negligible for sparse canopies. Therefore, the total reflected shortwave irradiance (RR_S) was calculated as

$$RR_S = R_S\left[\alpha_C f_{DHC} + \alpha_S \tau_C\left(1 - f_{DHC}\right)\right] \quad [10]$$

where α_C and α_S are the canopy and soil albedo, respectively, and f_{DHC} is the downward hemispherical–canopy view factor (i.e., the fraction of canopy appearing to a radiometer with a downward hemispherical view). Procedures for calculating f_{DHC}, given in Appendix 3, were developed in this study for a geometric approach where the canopy row was modeled as an elliptical hedgerow. Briefly, f_{DHC} is calculated in a similar manner to f_{SC}, where f_{DHC} is a function of solar zenith and azimuth angles, canopy height and width, row spacing, and also radiometer height and perpendicular distance from the canopy row center. The first term in the brackets of Eq. [10] ($\alpha_C f_{DHC}$) is the fraction of shortwave radiation reflected from the canopy. The second term in the brackets of Eq. [10] [$\alpha_S \tau_C (1 - f_{DHC})$] is the fraction of shortwave radiation reflected directly from the soil, which originates as TR_S (i.e., both shortwave radiation striking the soil directly and shortwave radiation transmitted through the canopy). Therefore, $(1 - f_{DHC})$ includes both sunlit and shaded soil components. If the clumping index is used instead of the geometric approach, then $f_{DHC} = f_{SC} = 1.0$ and Eq. [10] becomes $RR_S = R_S \alpha_C$.

The α_C term is comprised of reflectance components similar to τ_C in Eq. [2] and is calculated as

$$\alpha_C = F_{PAR}\left(W_{DIR,PAR}\rho_{C,DIR,PAR} + W_{DIFF,PAR}\rho_{C,DIFF,PAR}\right) + F_{NIR}\left(W_{DIR,NIR}\rho_{C,DIR,NIR} + W_{DIFF,NIR}\rho_{C,DIFF,NIR}\right) \quad [11]$$

where $\rho_{C,DIR,PAR}$ and $\rho_{C,DIR,NIR}$ are the canopy reflectance in the direct-beam PAR and NIR wavelengths, respectively, and $\rho_{C,DIFF,PAR}$ and $\rho_{C,DIFF,NIR}$ are the canopy reflectance in the diffuse PAR and NIR wavelengths, respectively. The $\rho_{C,DIR,PAR}$ term was calculated following Campbell and Norman (1998):

$$\rho_{C,DIR,PAR} = \frac{\rho_{C,PAR}^{*} + \xi_{PAR}}{1 + \xi_{PAR}\rho_{C,PAR}^{*}} \quad [12]$$

where

$$\xi_{PAR} = \frac{\left(\rho_{C,PAR}^{*} - \rho_{S,PAR}\right)}{\left(\rho_{C,PAR}^{*}\rho_{S,PAR} - 1\right)} \times \exp\left(-2\sqrt{\zeta_{PAR}} K_{BE}\eta LAI\right) \quad [13]$$

The nonrandom spatial distribution of row crops for reflectance is accounted for by η in Eq. [13] (i.e., similar to transmittance in Eq. [3]). The $\rho_{C',DIR,NIR}$ term in Eq. [11] was calculated by replacing ζ_{PAR} with ζ_{NIR} in Eq. [5] (resulting in $\rho_{C',NIR}^{*}$ in Eq. [4], [5], and [12]), ζ_{PAR} with ζ_{NIR} in Eq. [13] (resulting in ξ_{NIR} in Eq. [12] and [13]), and $\rho_{S',PAR}$ with $\rho_{S',NIR}$ in Eq. [12]. The $\rho_{C',DIFF,PAR}$ and

Table 1. Instrumentation used in irradiance measurements to optimize ellipsoid leaf angle distribution function parameter (X_E) and leaf absorption (ζ) for photosynthetically active radiation (PAR) and near-infrared radiation.

Variable	Instrument	Crops (no. of instruments)
Incident solar irradiance (R_S)†	Eppley PSP‡	corn (2), sorghum (2), cotton (2)
Incident PAR (IPAR)†	LI-COR LI-190 SA§	corn (1), sorghum (1), cotton (1)
Transmitted solar irradiance (TR_S)	Decagon tube solarimeter¶	corn (4), sorghum (4)
Transmitted PAR (TPAR)	LI-COR LQ§	corn (4), sorghum (4)
	LI-COR LI-191§	cotton (3)
Reflected solar irradiance (RR_S)	Eppley B&W 8–48‡	corn (2), sorghum (2)
	Kipp & Zonen CM14#	cotton (2)
Reflected PAR (RPAR)	LI-COR LI-190 SA§	corn (2), sorghum (2)
	LI-COR LI-190 SB§	cotton (2)

† Incident measurements were taken at a nearby grass reference site.
‡ Eppley Laboratory, Newport, RI.
§ LI-COR Biosciences, Lincoln, NE.
¶ Decagon Devices, Pullman, WA.
# Kipp & Zonen USA, Bohemia, NY.

$\rho_{C'DIFF,NIR}$ components in Eq. [11] are calculated by numerically integrating $\rho_{C'DIR,PAR}$ and $\rho_{C'DIR,NIR}$ over a half-sphere (i.e., the same as for $\tau_{C,DIFF,PAR}$ and $\tau_{C,DIFF,NIR}$). As with transmittance, calculating the reflectance in the different spectral bands (PAR and NIR) requires changing only two parameters (ζ_{PAR} vs. ζ_{NIR} and $\rho_{S,PAR}$ vs. $\rho_{S,NIR}$).

Soil albedo (α_S) includes both PAR and NIR spectra, calculated as

$$\alpha_S = F_{PAR}\rho_{S,PAR} + F_{NIR}\rho_{S,NIR} \quad [14]$$

where $\rho_{S,PAR}$ and $\rho_{S,NIR}$ are soil reflectance in the PAR and NIR wavelengths, respectively (assumed to be 0.15 and 0.25).

Reflected PAR (RPAR) was calculated as

$$\begin{aligned} \text{RPAR} = {} & \\ & R_S\left(4.602F_{PAR}\right) \\ & \times\left[\rho_{C,PAR}f_{DHC} + \rho_{S,PAR}\tau_{C,PAR}\left(1-f_{DHC}\right)\right] \end{aligned} \quad [15]$$

where

$$\rho_{C,PAR} = F_{PAR}\left(W_{DIR,PAR}\rho_{C,DIR,PAR} + W_{DIFF,PAR}\rho_{C,DIFF,PAR}\right) \quad [16]$$

MATERIALS AND METHODS

Field Measurements

All measurements were obtained at the USDA-ARS Conservation and Production Research Laboratory, Bushland, TX (35°11′ N, 102°6′ W, 1170-m elevation above mean sea level). The climate is semiarid, with an evaporative demand of about 2600 mm yr^{-1} (Class A pan evaporation) and precipitation averaging 470 mm yr–1. The soil is a Pullman clay loam (a fine, mixed, superactive, thermic Torrertic Paleustoll) with slow permeability, having a dense Bt1 layer from about the 0.15- to 0.40-m depth and a calcic horizon that begins at the 1-m depth (NRCS, 2011).

The crops evaluated were grain corn (1989 season), grain sorghum (1988 season), and upland cotton (2008 season). Cultural practices were similar to those used for high-yield production in the southern High Plains. All crops were planted in east–west raised beds spaced 0.8 m apart and were irrigated with lateral-move sprinklers. Corn and sorghum had planting densities of 6.0 and 16.0 plants m^{-2}, respectively, and the cotton planting density was 15.8 plants m^{-2}. All crops were irrigated to fully meet the crop water demand (i.e., an irrigation rate at 100% of full crop ET). Steiner et al. (1991), Tolk et al. (1995), and Howell et al. (1997) gave additional information on the corn and sorghum experiments. Agronomic and management practices for the cotton season were similar to those described by Howell et al. (2004).

Instrumentation and measured irradiance fluxes are summarized in Table 1. All measurements were sampled every 6 s and averaged to 0.5 h (0.25 h in 2008). The 0.5-h averages are reported as the midpoint of the average (e.g., 0930 to 1000 h is reported as 0945 h). Measurements were obtained during most of the crop seasons for each crop, from shortly after emergence to leaf senescence, and included a wide range of h_C and LAI values (Fig. 2). Measurements were excluded when θ_S was >80°, which is outside the valid range of Eq. [6] for calculating K_{BE} (Campbell and Norman, 1998), or when instruments were cleaned and checked for levelness, or when other equipment maintenance or activity occurred in the vicinity of the instruments, which were located at large weighing lysimeters.

Plant measurements and destructive samples were taken periodically at key growth stages at three field locations from destructive sample areas of 1.0 to 1.5 m^2. Green leaf area was measured with a LI-COR leaf area meter (Model LI-3100, LI-COR Biosciences, Lincoln, NE), and the meter accuracy was verified periodically with a 0.005-m^2 standard disk. The LAI and h_C were related to growing degree days by linear interpolation so that these variables could be estimated between measurement dates (Fig. 2).

Parameter Optimization

The Campbell and Norman (1998) procedure requires three parameters (X_E, ζ_{PAR}, and ζ_{NIR}) that were not measured in this study, and a sensitivity analysis indicated that TR_S, TPAR, RR_S, and RPAR were sensitive to these parameters when LAI was >2.0 (Colaizzi et al., 2012). Because X_E depends on the canopy architecture, it is species specific (Campbell and Norman, 1998). To restate the rationale for optimizing X_E, ζ_{PAR}, and ζ_{NIR}, ranges of X_E values have been established for corn and grain sorghum, but these have not been widely investigated for varying canopy cover, particularly where additional procedures were used to account for a nonrandom spatial distribution of the vegetation. Furthermore, although previous studies have investigated leaf angles of cotton (e.g., Thanisawanyangkura et al., 1997), few studies have directly related these to the X_E parameter. A similar argument would apply

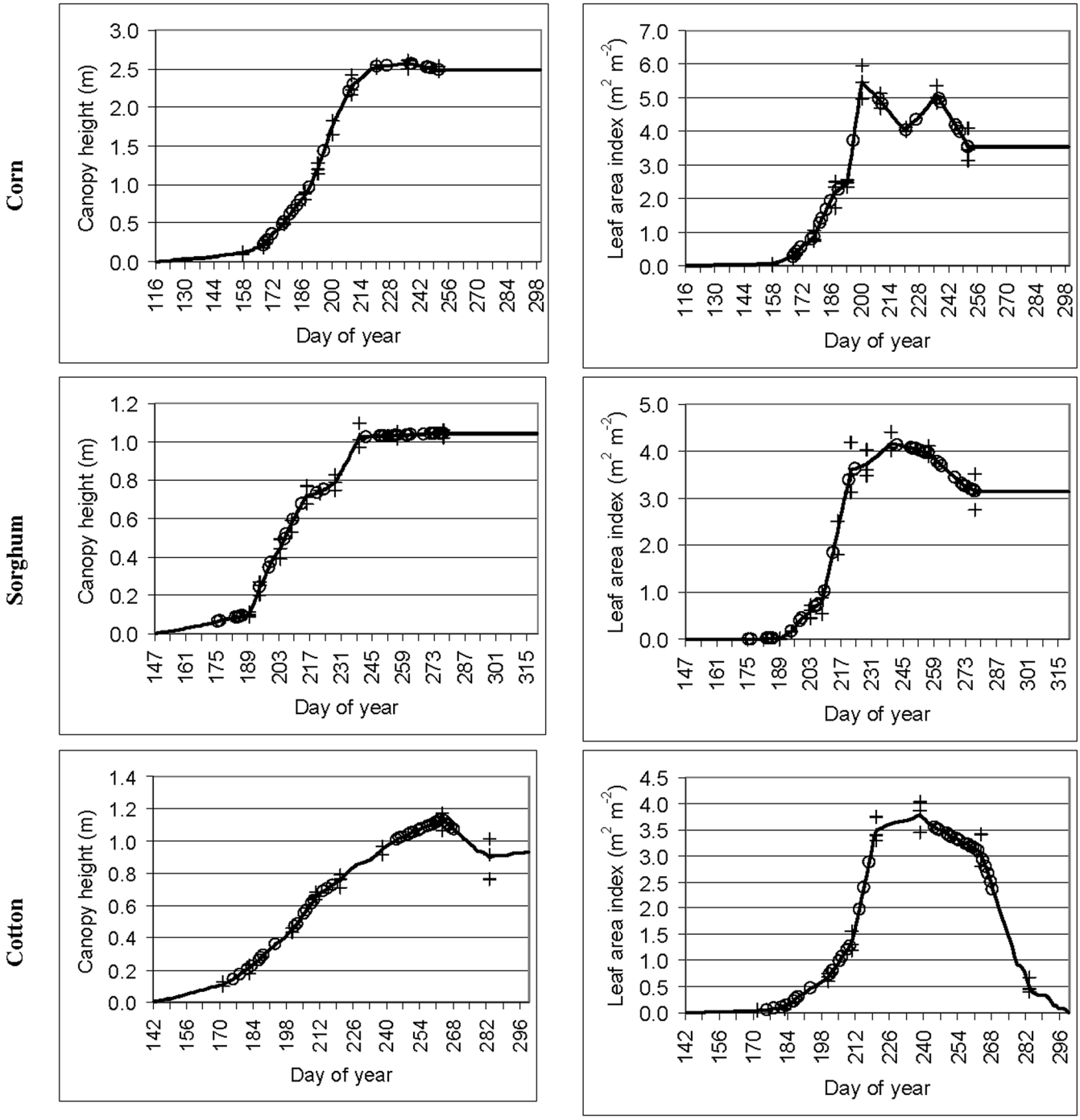

Fig. 2. Canopy height and leaf area index of corn, sorghum, and cotton: field measurements (+), linear interpolation between field measurements as a function of growing degree days (solid line), and days used for ellipsoid leaf angle distribution function parameter, leaf absorption for photosynthetically active radiation, and leaf absorption for near-infrared radiation (ζ_{NIR}) parameter optimization (O).

to ζ_{PAR} and ζ_{NIR}, which have also been shown to vary with species (e.g., Gausman and Allen, 1973). Also, no studies have assessed whether these parameters are distinctly identifiable (i.e., do not suffer from parameter correlation; Yeh, 1986) when used with models that account for a nonrandom spatial distribution of the vegetation. Accordingly, the X_E, ζ_{PAR}, and ζ_{NIR} parameters were estimated based on a crop-specific optimization procedure, which consisted of calculating model agreement between calculated and measured irradiance fluxes (TR_S, TPAR, RR_S, and RPAR) in terms of an objective function. The optimization procedure consisted of maximizing the objective function, which was defined as

$$\Phi(\beta,\chi)=\frac{1}{4}\sum_{j=1}^{4}E_{Cj}(\beta,\chi) \quad [17]$$

where E_{Cj} is the modified coefficient of model efficiency (Legates and McCabe, 1999) of the jth irradiance flux (i.e., TR_S, TPAR, RR_S, or RPAR), β are the vectors of optimized parameters (X_E, ζ_{PAR}, and ζ_{NIR}), and χ are the vectors of independent variables measured at time t_i required for estimation of the jth irradiance flux (e.g., LAI, h_C, R_S, etc.), and

$$E_{Cj}=1.0-\frac{\sum_{i=1}^{n_j}\left|M\left(t_{i,j}\right)-C\left(\beta,\chi_{i,j}\right)\right|}{\sum_{i=1}^{n_j}\left|M\left(t_{i,j}\right)-\overline{M}_j\right|} \quad [18]$$

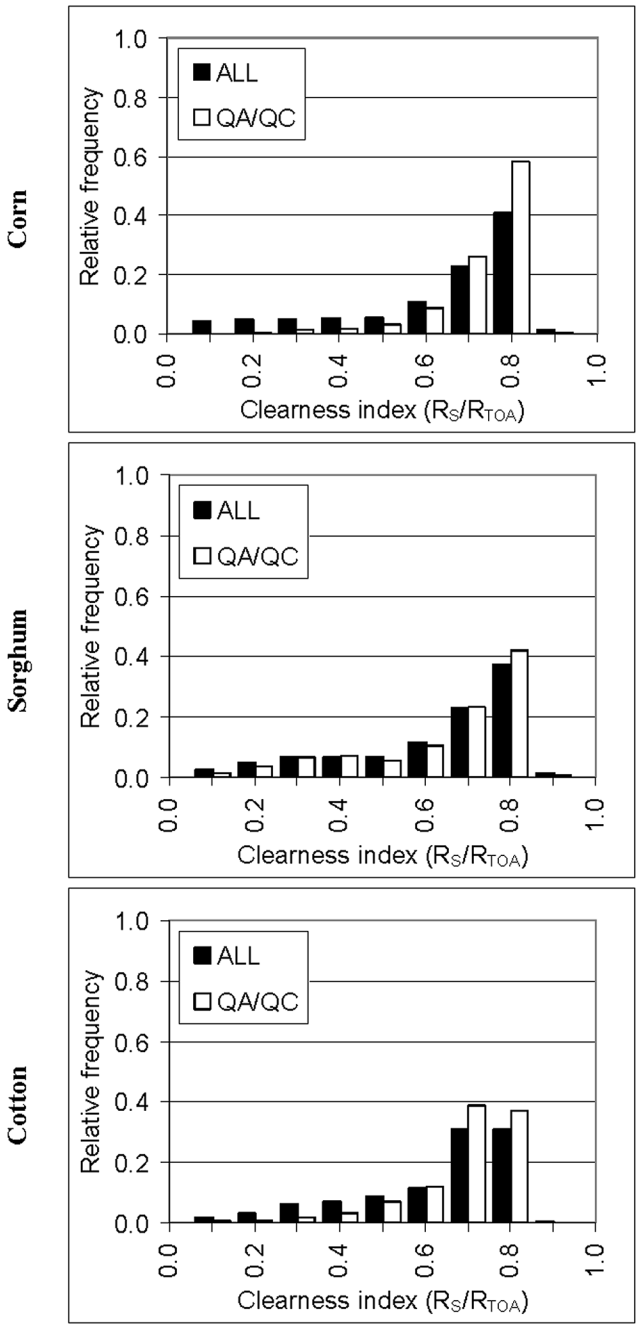

Fig. 3. Relative frequency of the sky clearness index for the entire season (ALL) and measurement days following data quality assurance and quality control (QA/QC) for corn, sorghum, and cotton data sets used in ellipsoid leaf angle distribution function parameter, leaf absorption for photosynthetically active radiation, and leaf absorption for near-infrared radiation parameter optimization.

where $M(t_{i,j})$ is the measured jth irradiance flux with n_j measurements at time t_i, $C(\beta,\chi_{i,j})$ is the corresponding calculated value, and $\overline{M_j}$ is the mean of the jth measured irradiance flux, i.e.,

$$\overline{M_j} = \frac{1}{n_j}\sum_{i=1}^{n_j} M\left(t_{i,j}\right) \quad [19]$$

Values of model efficiency are delineated by $-\infty < E_{Cj} \le 1.0$, with greater E_{Cj} values indicating better model agreement. If $E_{Cj} = 0$, then the mean of the measured values ($\overline{M}$) is as good an estimate as the model, but if E_{Cj} is <0, then $\overline{M}$ is actually a better estimate than the model. Legates and McCabe (1999) argued that E_{Cj} as defined here was less sensitive to outliers than the original Nash and Sutcliffe (1970) coefficient of model efficiency because the difference terms in E_{Cj} are not squared. Although the objective function can be defined using other model evaluation statistics (Moriasi et al., 2007), the modified coefficient of model efficiency was selected because it is based on the commonly used Nash and Sutcliffe (1970) model efficiency term, which has been reported to be a superior objective function for optimizing parameters (Servat and Dezetter, 1991).

Parameter values were optimized using the Microsoft Excel Solver add-in feature (Microsoft Office Excel 2003 SP3, Microsoft Corp., Redland, WA) to maximize the objective function, which uses the generalized reduced gradient method (Lasdon et al., 1978) with forward differencing. Iterations were run until the maximum scaled relative change in the objective function was <0.0001. The final parameter values were determined for each crop using both the clumping index and elliptical hedgerow approaches. The optimization was subject to parameter constraints that included a wide range of all physically plausible values (i.e., $0.1 \le X_E \le 5.2$, $0.70 \le \zeta_{PAR} \le 0.90$, and $0.10 \le \zeta_{NIR} \le 0.30$). Campbell and Norman (1998, Table 15.1) gave X_E values for various crops that were between 0.67 and 4.10, and gave ζ_{PAR} as 0.80 to 0.85 and ζ_{NIR} as 0.15 to 0.20. The final parameter values were verified by contour plots of objective function response surfaces in the X_E–ζ_{PAR}, X_E–ζ_{NIR}, and ζ_{PAR}–ζ_{NIR} parameter spaces, where X_E was varied in increments of 0.05 and ζ_{PAR} and ζ_{NIR} were varied in increments of 0.01.

RESULTS AND DISCUSSION

Measurements of irradiance fluxes (TR_S, TPAR, RR_S, and RPAR) used to optimize the X_E, ζ_{PAR}, and ζ_{NIR} parameters were obtained for a large range of h_C and LAI values for each crop; this was a much larger range than other studies of canopy radiative transfer models reviewed here (Fig. 2). Vegetation was considered to have a nonrandom spatial distribution when plant width was less than the crop row spacing ($w_C < r_V$, where r_V = 0.8 m). The corn and sorghum w_C and h_C were approximately equal, but for cotton, $w_C \sim 0.75h_C$ (data not shown). Therefore, a nonrandom spatial distribution of vegetation was inferred when h_C < 0.8 m for corn and sorghum and h_C < 1.0 m for cotton. This included 10 out of 22 measurement days for corn, 15 out of 33 measurement days for sorghum, and 17 out of 36 measurement days for cotton. Measurements also included days later in the season when leaves began to senesce, as indicated by a decreasing LAI. Corn measurements included 4 d during the middle of the season with minor hail damage (when LAI decreased from Day of the Year [DOY] 200–221), but the crop appeared to recover as LAI increased again by DOY 236 before decreasing due to leaf senescence later in the season.

The semiarid climate of the study location resulted in mostly clear skies during each crop season, which implied that beam irradiance dominated over diffuse irradiance in the available data. Overall sky conditions and data representativeness were assessed by comparing the frequency distributions of the sky clearness index for the entire season (ALL) and measurement days following data quality assurance and quality control (QA/QC) for each crop (Fig. 3). The clearness index is defined as R_S/R_{TOA} (e.g., Jacovides et al., 2007), where R_{TOA} is the top-of-atmosphere global irradiance (calculated following the Task

Table 2. Corn statistical parameters of agreement of measured and calculated shortwave irradiance flux (transmitted solar irradiance [TR_S], transmitted photosynthetically active radiation [TPAR], reflected solar irradiance [RR_S], and reflected photosynthetically active radiation [RPAR]) and maximized objective function (Φ) using optimized parameters.

Parameter†	TR_S	TPAR	RR_S	RPAR
	W m^{-2}	μmol m^{-2} s^{-1}	W m^{-2}	μmol m^{-2} s^{-1}
n	603	603	603	603
Measured mean	310.2	470.2	117.8	73.0
Measured SD	236.3	466.3	40.4	51.5
Clumping index, X_E‡ = 1.02, ζ_{PAR}§ = 0.85, ζ_{NIR}¶ = 0.20, Φ = 0.72				
Calculated mean	261.7	428.8	123.8	77.5
Calculated SD	255.5	515.9	40.4	61.6
E_C	0.69	0.79	0.70	0.69
RMSE	83.5	108.2	14.8	18.0
MAE	64.0	81.8	10.2	11.4
MBE	–48.5	–41.4	5.99	4.53
Elliptical hedgerow, X_E = 1.00, ζ_{PAR} = 0.85, ζ_{NIR} = 0.20, Φ = 0.75				
Calculated mean	271.1	474.3	118.8	69.0
Calculated SD	261.7	542.7	37.2	46.3
E_C	0.71	0.79	0.74	0.77
RMSE	78.8	109.4	11.4	12.7
MAE	59.9	83.8	8.84	8.28
MBE	–39.1	4.1	1.01	–3.99

† E_C, coefficient of model efficiency; MAE, mean absolute error; MBE, mean bias error.
‡ X_E, ellipsoid leaf angle distribution function parameter.
§ ζ_{PAR}, leaf absorption for photosynthetically active radiation.
¶ ζ_{NIR}, leaf absorption for near-infrared radiation.

Table 3. Grain sorghum statistical parameters of agreement of measured and calculated shortwave irradiance flux (transmitted solar irradiance [TR_S], transmitted photosynthetically active radiation [TPAR], reflected solar irradiance [RR_S], and reflected photosynthetically active radiation [RPAR]) and maximized objective function (Φ) using optimized parameters.

Parameter†	TR_S	TPAR	RRs	RPAR
	W m^{-2}	μmol m^{-2} s^{-1}	W m^{-2}	μmol m^{-2} s^{-1}
n	685	685	615	615
Measured mean	276.4	460.3	113.3	64.3
Measured SD	271.5	600.7	45.2	35.5
Clumping index, X_E‡ = 1.48, ζ_{PAR}§ = 0.82, ζ_{NIR}¶ = 0.20, Φ = 0.75				
Calculated mean	232.7	418.5	116.1	65.7
Calculated SD	274.5	586.7	44.7	43.8
E_C	0.77	0.87	0.72	0.66
RMSE	65.7	99.3	15.2	15.6
MAE	51.8	62.7	10.6	7.94
MBE	–43.7	–41.8	2.79	1.40
Elliptical hedgerow, X_E = 1.46, ζ_{PAR} = 0.82, ζ_{NIR} = 0.20, Φ = 0.77				
Calculated mean	233.5	432.7	114.8	64.0
Calculated SD	282.6	602.8	43.4	38.6
E_C	0.75	0.88	0.74	0.71
RMSE	68.5	89.8	13.9	12.2
MAE	55.2	59.5	9.84	6.87
MBE	–42.9	–27.7	1.58	–0.36

† E_C, coefficient of model efficiency; MAE, mean absolute error; MBE, mean bias error.
‡ X_E, ellipsoid leaf angle distribution function parameter.
§ ζ_{PAR}, leaf absorption for photosynthetically active radiation.
¶ ζ_{NIR}, leaf absorption for near-infrared radiation.

Committee on Standardization of Reference Evapotranspiration, 2005). Because atmospheric transmittance for clear skies is around 0.75 (Task Committee on Standardization of Reference Evapotranspiration, 2005), clear skies were inferred when $0.7 < R_S/R_{TOA} < 0.8$, which included approximately 80% of all measurements. For each crop, measurement days (QA/QC) had a slightly greater frequency of clear days than the entire season (ALL), but overall, the frequency distributions were similar. The lack of cloudy days resulted in global irradiance having a greater proportion (greater than ~70%) in the direct-beam component, resulting in greater emphasis on $\tau_{DIR,PAR}$ and $\tau_{DIR,NIR}$ in Eq. [2] and $\rho_{DIR,PAR}$ and $\rho_{DIR,NIR}$ in Eq. [11]. This is admittedly a limitation of the current study and would suggest that additional studies in more humid climates would be useful.

The optimized X_E, ζ_{PAR}, and ζ_{NIR} values were determined for the clumping index and elliptical hedgerow approaches for corn (Table 2), grain sorghum (Table 3), and cotton (Table 4). For each crop, both the clumping index and elliptical hedgerow approaches resulted in very similar optimized parameter values (±0.04 for X_E and ±0.005 for ζ_{PAR} and ζ_{NIR}), and both approaches resulted in similar model agreement for each irradiance flux (i.e., TR_S, TPAR, RR_S, and RPAR), where model agreement was assessed by E_{Cj} (i.e., Eq. [18]), root mean square error (RMSE), mean absolute error (MAE), and mean bias error. In all cases, E_{Cj} was > 0, indicating that the model was a better estimate than the mean of all measured values. Also, MAE was always at least 60% of RMSE, indicating that the data were relatively free of outliers (Legates and McCabe, 1999).

The optimized parameter values for corn were X_E = 1.02, ζ_{PAR} = 0.85, and ζ_{NIR} = 0.20 for the clumping index approach and X_E = 1.00, ζ_{PAR} = 0.85, and ζ_{NIR} = 0.20 for the elliptical hedgerow approach (Table 2). These values were within the ranges recommended by Campbell and Norman (1998, Table 15.1), where X_E was between 0.76 and 2.52, ζ_{PAR} was 0.80 to 0.85, and ζ_{NIR} was 0.15 to 0.20 for most green vegetation. The resulting X_E = 1.0 represents the spherical case of the ellipsoid LADF, which was recommended by Campbell and Norman (1998) if no other information is available on leaf angle. A more intuitive interpretation of X_E is in terms of the mean leaf inclination angle from the horizontal (θ_L), which can be approximated by

$$\theta_L \sim \cos^{-1}\left[K_{BE}\left(\theta_S = 0\right)\right] \quad [20]$$

where K_{BE} is calculated from Eq. [6] with θ_S = 0 (Campbell and Norman, 1998). Using this approximation, corn $\theta_L \sim 60°$ (Fig. 4), which was less than $\theta_L = 70°$ used by Doraiswamy et al. (2004) and others when retrieving corn LAI from satellite reflectance measurements. Although this discrepancy was minor, it may have been related to the inclusion of measurements with sparser canopy cover than other studies (e.g., the average corn LAI was at least around 1.0 in Doraiswamy et al., 2004), where leaves would be expected to have a more horizontal orientation for a sparse canopy than a denser canopy where larger plants with longer leaves would force a greater θ_L.

The optimized parameter values for grain sorghum were X_E = 1.48, ζ_{PAR} = 0.82, and ζ_{NIR} = 0.20 for the clumping index approach and X_E = 1.46, ζ_{PAR} = 0.82, and ζ_{NIR} = 0.20 for the elliptical hedgerow approach (Table 3). The X_E values were similar to the value given by Campbell and Norman (1998, Table 15.1), where X_E = 1.43 for grain sorghum. The

Table 4. Cotton statistical parameters of agreement of measured and calculated shortwave irradiance flux (transmitted photosynthetically active radiation [TPAR], reflected solar irradiance [RR_S], and reflected photosynthetically active radiation [RPAR]) and maximized objective function (Φ) using optimized parameters.

Parameter†	TPAR	RR_S	RPAR
	μmol m^{-2} s^{-1}	W m^{-2}	μmol m^{-2} s^{-1}
n	776	1339	1339
Measured mean	720.2	134.8	74.9
Measured SD	464.4	50.0	53.5
Clumping index, X_E‡ = 3.04, ζ_{PAR}§ = 0.83, ζ_{NIR}¶ = 0.14, Φ = 0.78			
Calculated mean	678.4	138.0	75.7
Calculated SD	527.6	52.0	57.5
E_C	0.75	0.79	0.79
RMSE	123.5	13.0	11.2
MAE	98.5	9.15	7.46
MBE	–41.8	3.20	0.74
Elliptical hedgerow, X_E = 3.00, ζ_{PAR} = 0.83, ζ_{NIR} = 0.14, Φ = 0.78			
Calculated mean	752.9	136.6	71.3
Calculated SD	530.8	52.3	51.5
E_C	0.73	0.80	0.78
RMSE	129.9	12.00	11.57
MAE	104.9	8.43	7.60
MBE	32.8	1.77	–3.63

† E_C, coefficient of model efficiency; MAE, mean absolute error; MBE, mean bias error.

‡ X_E, ellipsoid leaf angle distribution function parameter.

§ ζ_{PAR}, leaf absorption for photosynthetically active radiation.

¶ ζ_{NIR}, leaf absorption for near-infrared radiation.

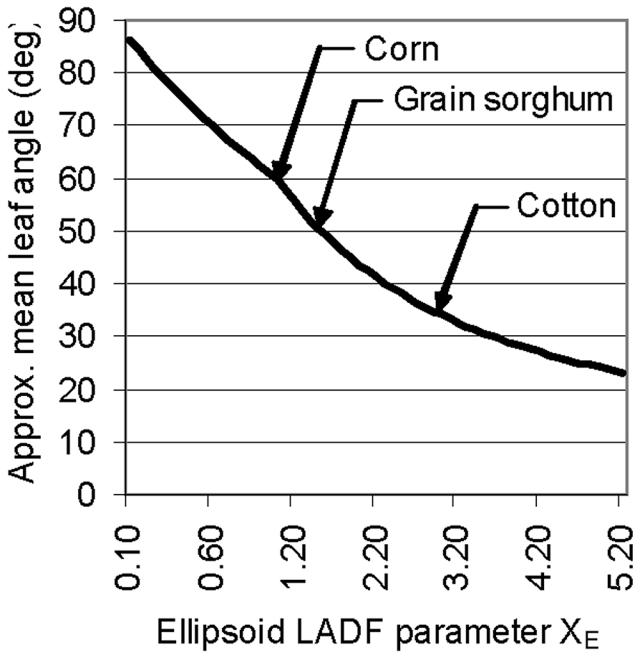

Fig. 4. Approximate mean leaf angle vs. the ellipsoid leaf angle distribution function (LADF) parameter (X_E), and resulting mean leaf angles for corn, grain sorghum, and cotton for optimized X_E values.

ζ_{PAR} value was similar and the ζ_{NIR} value was the same as for corn. The resulting optimized X_E values correspond to $\theta_L \sim 51°$, indicating that grain sorghum had a larger proportion of leaves oriented in the horizontal direction than corn (Fig. 4). Because both crops have a somewhat similar canopy architecture but grain sorghum is a shorter crop with a narrower canopy width than corn, interrow foliage would be expected to be less dense for grain sorghum, resulting in more horizontal leaf angles.

The optimized parameter values for cotton were $X_E = 3.04$, $\zeta_{PAR} = 0.83$, and $\zeta_{NIR} = 0.14$ for the clumping index approach and $X_E = 3.00$, $\zeta_{PAR} = 0.83$, and $\zeta_{NIR} = 0.14$ for the elliptical hedgerow approach (Table 4). The $X_E = 3.0$ corresponds to $\theta_L \sim 34°$ (Fig. 4), which was consistent with Thanisawanyangkura et al. (1997), who reported cotton θ_L averaged 36, 33, and 36° for morning, midday, and afternoon solar zenith angles, respectively, for a range of LAI (0.12, 1.09, and 2.84). The changing θ_L of cotton is the result of diaheliotropism, where leaves tend to orient themselves normal to the sun to maximize radiation interception, which is discussed further below.

The optimization procedure resulted in identifiable X_E, ζ_{PAR}, and ζ_{NIR} values for each crop (Fig. 5). The response surface of the objective function for each crop was plotted in the X_E–ζ_{PAR}, X_E–ζ_{NIR}, and ζ_{NIR}–ζ_{PAR} parameter spaces using the elliptical hedgerow approach (the clumping index plots were similar; data not shown). Each optimized solution (shown as × in Fig. 5) was enclosed by contours in the parameter space, and the contours were monotonically decreasing in all directions away from the optimized solution within the limits of each parameter space. Hence, the maximization of the objective function appeared to avoid parameter identification problems by simultaneously fitting the three parameters (Yeh, 1986).

The use of a species-specific X_E parameter value for sorghum and cotton improved model agreement, i.e., increased the objective function value, compared with assuming $X_E = 1.0$, which was recommended by Campbell and Norman (1998) if no other information on leaf angle for a particular species was available. For example, the objective function for cotton would have been reduced from 0.78 to 0.68 if $X_E = 1.0$ had been used instead of $X_E = 3.0$ (Fig. 5). From Eq. [20], $X_E = 1.0$ would result in $\theta_L \sim 60°$, implying more erect cotton leaves than $X_E = 3.0$ (and $\theta_L \sim 34°$), and the assumption of more erect leaves would have resulted in overestimates of TR_S, TPAR, and RPAR and underestimates of RR_S. This result agreed with Thanisawanyangkura et al. (1997; see their Fig. 4), where $\theta_L > 60°$ was far less frequent for small (LAI = 0.12), medium (LAI = 1.09), and full (LAI = 2.84) cotton canopies. The objective function in this study was much less sensitive to $X_E > 1.5$, however, which implies that the cotton canopy contained a greater proportion of leaves that were oriented more horizontally and also that the leaf angle distribution had greater variability for θ_L less than ~50°, which would be expected for a diaheliotropic species as θ_S varies. This result also agreed with Thanisawanyangkura et al. (1997); although their leaf angle distribution frequency for medium to full cotton canopies appeared independent of θ_S, their leaf angle distribution was fairly uniform and had the largest frequencies for $20° < \theta_L < 60°$, and this was also within the range of θ_S in their study. In the current study, the objective function sensitivity to X_E for grain sorghum was somewhat similar to cotton, but the grain sorghum objective function decreased more rapidly as X_E increased compared with cotton.

In contrast to X_E, ζ_{PAR} was not as sensitive to the crop species in that it had similar optimized values for each crop (i.e., 0.85, 0.82, and 0.83 for corn, grain sorghum, and cotton, respectively). The greater consistency of ζ_{PAR} values for different species was

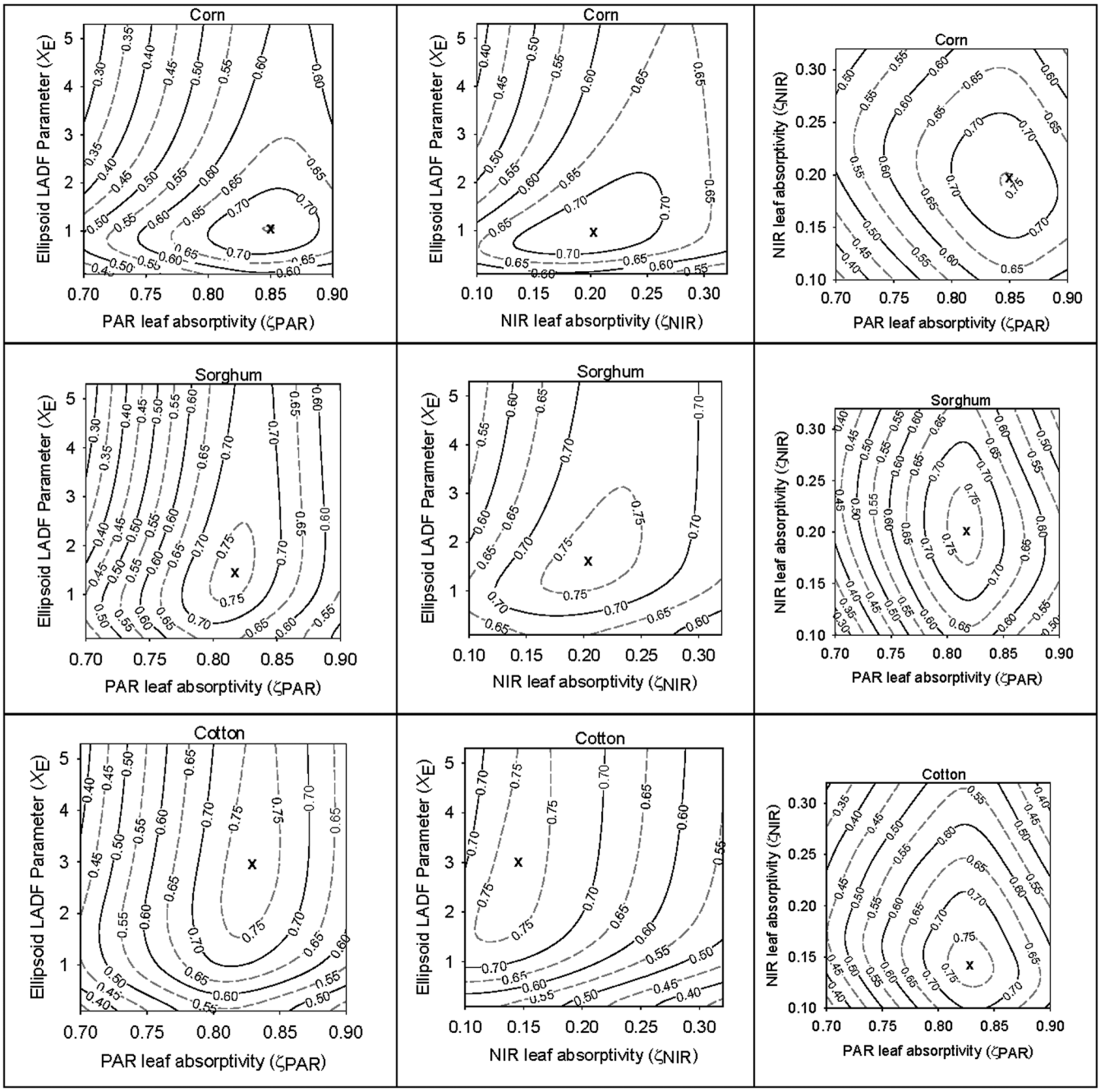

Fig. 5. Objective function response surfaces in the ellipsoid leaf angle distribution function (LADF) parameter (X_E)–leaf absorption for photosynthetically active radiation (ζ_{PAR}) (left), X_E– leaf absorption for near-infrared radiation (ζ_{NIR}) (center), and ζ_{NIR}–ζ_{PAR} (right) parameter spaces. The optimized solutions are shown as ×.

despite the objective function being rather sensitive to this parameter for each crop (Fig. 5); however, ζ_{NIR} was 0.20 for corn and grain sorghum (C_4 plants) and 0.14 for cotton (a C_3 plant). This may have been related to differing leaf CO_2 concentrations resulting from the metabolic pathways, which has been exploited in NIR spectroscopy (e.g., Clark et al., 1995). The objective function was more sensitive to ζ_{PAR} than ζ_{NIR}. This was probably a consequence of the available irradiance flux measurements being weighted more in the PAR wavelengths because only TR_S and RR_S were dependent on ζ_{NIR} but all fluxes were dependent on ζ_{PAR}. The optimized ζ_{PAR} and ζ_{NIR} values were within the range suggested by Campbell and Norman (1998) (i.e., $0.80 \le \zeta_{PAR} \le 0.85$ and $0.15 \le \zeta_{NIR} \le 0.20$), although cotton ζ_{NIR} was slightly less at 0.14. The use of optimized ζ_{PAR} and ζ_{NIR} values improved model agreement compared with selecting, say, a ζ_{PAR} value of either 0.80 or 0.85 for sorghum or cotton, a ζ_{NIR} value of 0.15 for corn or sorghum, or 0.20 for cotton.

CONCLUSIONS

Line (planar) and hemispherical radiometer view factors were developed for row crops with partial vegetation cover, where the view factors were derived for a crop row modeled as an elliptical hedgerow. The view factors were used with an existing radiative transfer model (Campbell and Norman, 1998) to estimate transmitted and reflected shortwave radiation. With this approach, the model requires only location longitude and latitude, local time, R_S, h_C, w_C, LAI, $\rho_{S,PAR}$, $\rho_{S,NIR}$, X_E, ζ_{PAR}, and ζ_{NIR}. Crop-specific X_E, ζ_{PAR}, and ζ_{NIR} values were optimized by maximizing an

objective function that was based on the Legates and McCabe (1999) modified coefficient of model efficiency between model output and measurements of transmitted and reflected shortwave irradiance. Parameters were optimized for corn, grain sorghum, and cotton with wide ranges of canopy cover. The optimization procedure used both the elliptical hedgerow view factor approach and the commonly used, semiempirical clumping index approach to account for the nonrandom spatial distribution of row crop vegetation. The final optimized parameter values were $X_E = 1.0$, $\zeta_{PAR} = 0.85$, and $\zeta_{NIR} = 0.20$ for corn; $X_E = 1.5$, $\zeta_{PAR} = 0.82$, and $\zeta_{NIR} = 0.20$ for grain sorghum; and $X_E = 3.0$, $\zeta_{PAR} = 0.83$, and $\zeta_{NIR} = 0.14$ for cotton. Hence, the only parameters that changed appreciably were X_E and ζ_{NIR}, whereas ζ_{PAR} was very similar for each crop. The final optimized values were insensitive to the choice of clumping index or elliptical hedgerow approach and were within ±0.04 for X_E and ±0.005 for ζ_{PAR} and ζ_{NIR}. The elliptical hedgerow approach, however, resulted in slightly greater maximum objective function values compared with the clumping index approach for corn and sorghum. The objective function for cotton was insensitive to X_E values >1.5 but more sensitive to smaller X_E values, a result probably related to diaheliotropism. All optimized parameters were distinctly identifiable, however, and no parameter correlation was observed for any crop. The optimized X_E values and approximate corresponding leaf inclination angles agreed very well with existing values in the literature for each crop, and the optimized ζ_{PAR} and ζ_{NIR} values were generally within the range suggested by Campbell and Norman (1998). This suggests that the radiative transfer model was robust for different row crops having dissimilar canopy architecture. The optimized parameters were applied to the radiative transfer model, and model performance was compared and a sensitivity analysis was conducted using the clumping index and elliptical hedgerow approaches for a different data set across a wide range of vegetation cover (Colaizzi et al., 2012).

APPENDIX 1
Direct-Beam and Diffuse Weighing Factors for Photosynthetically Active and Near-Infrared Radiation

The direct-beam weighing factors for the PAR and NIR wavelengths ($W_{DIR,PAR}$ and $W_{DIR,NIR}$, respectively) were calculated in a manner similar to Weiss and Norman (1985) as

$$W_{DIR,PAR} = \left(\frac{R_{SO,DIR}}{R_{SO}}\right) a \left(\frac{R_S}{R_{SO}}\right)^b \quad [A1]$$

$$W_{DIR,NIR} = \left(\frac{R_{SO,DIR}}{R_{SO}}\right) c \left(\frac{R_S}{R_{SO}}\right)^d \quad [A2]$$

where $R_{SO,DIR}$ and R_{SO} (W m^{-2}) are the direct-beam and global incoming solar irradiance for clear skies, respectively (calculated following Task Committee on Standardization of Reference Evapotranspiration, 2005), where a simple empirical model accounts for atmospheric turbidity and moisture), R_S is measured incoming solar irradiance (W m^{-2}), and a, b, c, and d are empirical constants. The diffuse weighing factors are the unit complements of the direct-beam weighing factors (i.e., $W_{DIFF,PAR} = 1.0 - W_{DIR,PAR}$ and $W_{DIFF,NIR} = 1.0 - W_{DIR,NIR}$).

The empirical constants were determined at the study location as $a = 1.034$, $b = 2.234$, $c = 1.086$, and $d = 2.384$. These constants were determined based on measurements of total incoming and diffuse R_S (Eppley PSP, Eppley Laboratory, Newport, RI) and total incoming and diffuse PAR (LI-COR LI-190-SA, LI-COR Biosciences, Lincoln, NE) during 1993 for a wide range of sky conditions (i.e., $0.1 \le R_S/R_{SO} \le 1.0$). Diffuse irradiance was measured using the same instruments as for total incoming irradiance but with shadow band shading devices installed (Eppley SBS, Eppley Laboratory). The shadow band for R_S had a radius and width of 318 and 75 mm, respectively, and the shadow band for PAR had a radius and width of 80 and 13 mm, respectively. The shadow bands were adjusted each week for solar declination and corrected for diffuse irradiance obscured by the shadow band using the method of Muneer and Zhang (2002), which was found to have less error across a wide range of sky conditions than three other commonly used methods (López et al., 2004). Direct beam components were derived as the difference between the total and diffuse components, and the NIR wavelengths were derived as the difference between the global and PAR wavelengths. The modified coefficient of model efficiency (E_C) (Legates and McCabe, 1999) was determined for calculated (using Eq. [A1] or [A2]) vs. measurement-derived $W_{DIR,PAR}$ and $W_{DIR,NIR}$, respectively. The empirical constants used in Eq. [A1] and [A2] were optimized using the Microsoft Excel Solver add-in feature, where E_C was maximized using the generalized reduced gradient method (Lasdon et al., 1978) with forward differencing.

The resulting empirical constants were tested by comparing the calculated $W_{DIR,PAR}$ and $W_{DIR,NIR}$ with those derived from total and diffuse R_S and PAR during 1992, where $0.2 \le R_S/R_{SO} \le 1.0$. The resulting RMSEs (calculated vs. measurement derived) were 0.130 (24% of the measured mean) and 0.136 (23% of the measured mean) for $W_{DIR,PAR}$ and $W_{DIR,NIR}$, respectively. Model agreement was similar to that reported in other studies using models based on a simple clearness index (i.e., R_S/R_{SO}) (e.g., Weiss and Norman, 1985; Jacovides et al., 2007).

APPENDIX 2
Solar Canopy View Factor

The solar canopy view factor (f_{SC}) is defined as the line or planar fraction of canopy visible from the direction of the sun. For this study, f_{SC} was derived based on simple geometric relations where crop rows were modeled as elliptical hedgerows, where the spatial distribution of vegetation is nonrandom in directions that are not parallel to the crop row but uniform in the direction parallel to the row. Therefore, for hedgerow geometry, the line view extended in the direction parallel to the rows is equivalent to the planar view. The only variables required to calculate f_{SC} are solar zenith and azimuth angles, canopy height and width, and row spacing. From Fig. A1, f_{SC} is defined as

$$f_{SC} \equiv \begin{cases} c_S/r_S & 0 \le c_S < r_S \\ 1.0 & c_S \ge r_S \end{cases} \quad [A3]$$

where c_S is the projected width of the canopy in a plane normal to incoming solar beam irradiance (m) and r_S is the projected canopy row spacing in a plane normal to incoming solar beam irradiance (m). In Fig. A1, the solar beams shown are projected

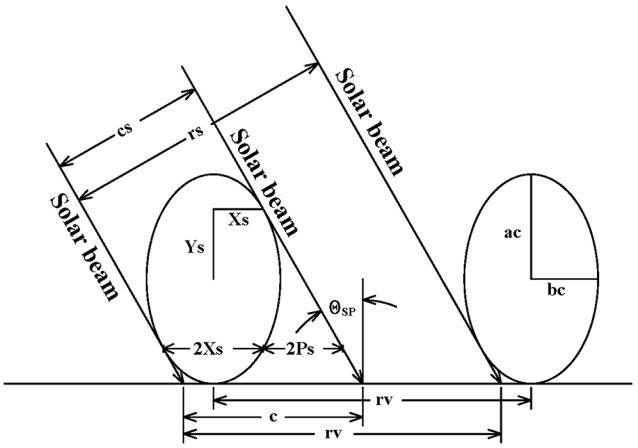

Fig. A1. Parameters used to calculate the solar canopy view factor.

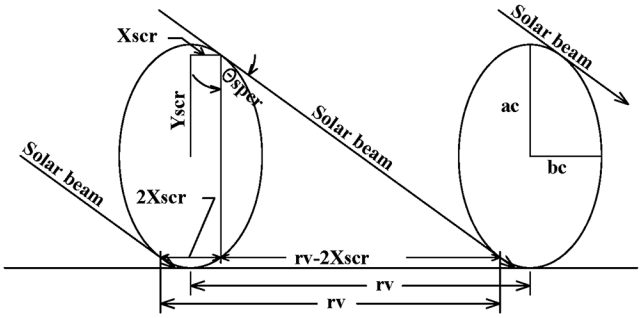

Fig. A2. Parameters used to calculate the critical projected solar zenith angle (θ_{SPCR}), where if the projected solar zenith angle $\theta_{SP} \geq \theta_{SPCR}$, then the solar canopy view factor f_{SC} = 1.0.

onto a plane normal to the ellipse cross-section, which forms a projected solar zenith angle (θ_{SP}), given as

$$\theta_{SP} = \tan^{-1}\left[\left(\tan\theta_S\right)\left|\sin\Phi_S\right|\right] \quad [A4]$$

where θ_S is the solar zenith angle and Φ_S is the solar azimuth relative to the crop row (i.e., $\Phi s = 0$ and $\pi/2$ rad when the sun is parallel and perpendicular to the crop row, respectively). It can be shown that

$$\frac{c_S}{r_S} = \frac{2X_S + 2P_S}{r_V} \quad [A5]$$

where $P_S = Y_S \tan\theta_{SP}$, X_S and Y_S are the horizontal and vertical distances (m), respectively, from the canopy ellipse origin to the tangent of the solar beam, and r_V is the row spacing (m). The values of X_S and Y_S are found by combining the equation of an ellipse with the slope (m_{SL}) of a line tangent to the ellipse (i.e., the solar beam), where the point (X_S,Y_S) is common to both equations:

$$\frac{X_S^2}{b_C^2} + \frac{Y_S^2}{a_C^2} = 1 \quad [A6]$$

and

$$m_{SL} = \frac{1}{\tan\theta_{SP}} = \frac{a_C^2}{b_C^2}\frac{X_S}{Y_S} \quad [A7]$$

where a_C and b_C are the major and minor ellipse semiaxes (m), respectively, $a_C = 1/2\ h_C$, where h_C is the canopy height (m), and $b_C = 1/2\ w_C$, where w_C is the canopy width (m). It can be shown that

$$X_S = \frac{b_C}{\sqrt{1 + \left(a_C^2/b_C^2\right)\tan^2\theta_{SP}}} \quad [A8]$$

$$Y_S = \frac{a_C^2}{b_C^2} X_S \tan\theta_{SP} \quad [A9]$$

There is a critical projected solar zenith angle (θ_{SPCR}) where f_{SC} = 1.0 if $\theta_{SP} \geq \theta_{SPCR}$. (analogous to $c_S \geq r_S$). At θ_{SPCR}, a solar beam will be tangent to adjacent ellipses (Fig. A2) and

$$\tan\theta_{SPCR} = \frac{r_V - 2X_{SCR}}{2Y_{SCR}} \quad [A10]$$

where X_{SCR} and Y_{SCR} are the horizontal and vertical distances, respectively, from the canopy ellipse origin to the tangent of the solar beam at θ_{SPCR}. Combining Eq. [A10] with Eq. [A6] and [A7], substituting X_{SCR}, Y_{SCR}, and θ_{SPCR} for X_S, Y_S, and θ_{SP}, respectively, and solving for X_{SCR} results in

$$X_{SCR} = \frac{2b_C^2}{r_V} \quad [A11]$$

If $X_S \leq X_{SCR}$, then $\theta_{SP} \geq \theta_{SPCR}$ and f_{SC} = 1.0.

APPENDIX 3

Downward Hemispherical Canopy View Factor and Upward-Line-Integrated Hemispherical Canopy View Factor

The downward hemispherical canopy view factor (f_{DHC}) is defined as the fraction of canopy visible from a point with a downward hemispherical view located over the canopy. It is commonly found with inverted dome radiometers that measure the reflected and net irradiance of vegetated surfaces. The derivation of f_{DHC} was based on crop rows modeled as elliptical hedgerows, in the same manner as f_{SC}. The variables required to calculate f_{DHC} are canopy height and width, row spacing, radiometer height from the soil surface, and radiometer perpendicular distance from the crop row center. From Fig. A3, f_{DHC} is calculated as

$$f_{DHC} = 1 - \frac{2}{\pi^2} \times \int_0^{\pi/2}\left\{\sum_{i=-N_R(\varphi_R)}^{i=+N_R(\varphi_R)} \max\left[0,\left(\theta_{R(1,i+1)} - \theta_{R(2,i)}\right)\right]\right\} d\varphi_R \quad [A12]$$

where θ_R is the radiometer zenith view angle (rad) that is tangent to each elliptical hedgerow, Φ_R is the radiometer azimuth view angle (rad) relative to the crop row (where 0 and $\pi/2$ rad are parallel and perpendicular, respectively, to the row), and N_R is the minimum integer number of interrows where bare soil is visible at a specific Φ_R for $0 \leq \theta_R < \pi/2$. Hence for each Φ_R, the fraction of bare soil is summed along the transect from $-N_R$ to $+N_R$. In Fig. A3, the sign convention for θ_R is negative to the left and positive to the right of the radiometer. If θ_R is sufficiently large, then $\theta_R(1,i+1) - \theta_R(2,i) < 0$ in Eq. [A12], meaning that no interrows (i.e., bare soil) will be visible, and the summation term is constrained to zero.

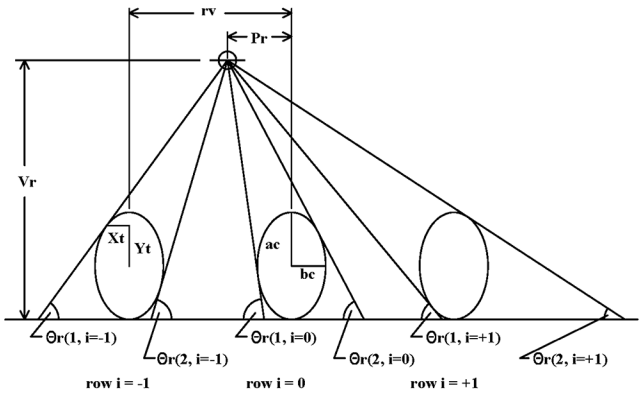

Fig. A3. Parameters used to calculate the downward hemispherical canopy view factor.

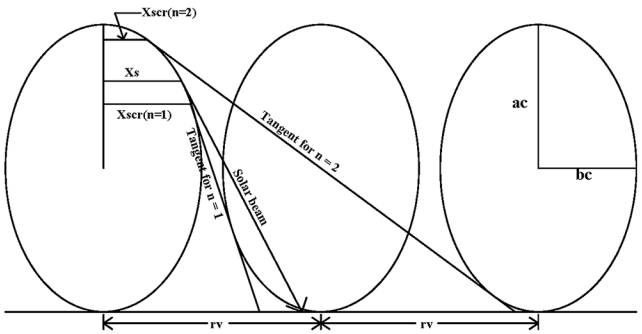

Fig. A5. Parameters used to calculate the multiple row factor for a solar beam through canopy rows modeled as elliptical hedgerows.

Computation of θ_R is done by considering the general case where θ_1 and θ_2 are the zenith angles of the left and right tangent lines, respectively, that extend from the radiometer to the elliptical hedgerow (Fig. A3). If the origin is located at the center of the ellipse, then one of the tangents is located at point (x_T,y_T) on the ellipse and the radiometer is located at point (x_R,y_R). Combining the equations for the line and the ellipse at (x_T,y_T), it can be shown that

$$\begin{aligned}&\left(y_R^2a_C^2-a_C^4\right)\tan^4\left(\theta_{1,2}\right)-\left(2x_Ry_Ra_C^2\right)\tan^3\left(\theta_{1,2}\right)\\&+\left(y_R^2b_{CR}^2+x_R^2a_C^2-2b_{CR}^2a_C^2\right)\tan^2\left(\theta_{1,2}\right)\\&-\left(2x_Ry_Rb_{CR}^2\right)\tan\left(\theta_{1,2}\right)+\left(x_R^2b_{CR}^2-b_{CR}^4\right)=0\end{aligned}\qquad[A13]$$

which is a quartic equation of the form $Ax^4 + Bx^3 + Cx^2 + Dx + E = 0$, and $y_R = V_R - a_C$, $x_R = P_R/\sin(\Phi_R)$, and $b_{CR} = b_C/\sin(\Phi_R)$, where P_R and V_R are the horizontal (perpendicular) and vertical distances (m), respectively, from the radiometer to the row center, and a_C and b_C are the semimajor and semiminor axes, respectively, of the ellipse. Solution of Eq. [A13] yields four roots; these are $\pm\tan(\theta_1)$ and $\pm\tan(\theta_2)$, where the location of the tangent line *relative to the radiometer* determines the sign (i.e., negative is left and positive is right), and the location of the tangent line *relative to the elliptical hedgerow* determines the angle (i.e., θ_1 is left and θ_2 is right). For multiple crop rows, P_R is simply replaced with $r_V i - P_R$.

Although f_{DHC} could be calculated by assigning a sufficiently high N_R in Eq. [A12] because interrows that are not visible are not summed, computational efficiency is greatly enhanced by reducing N_R to physically realistic values for each Φ_R. Therefore, N_R was calculated as

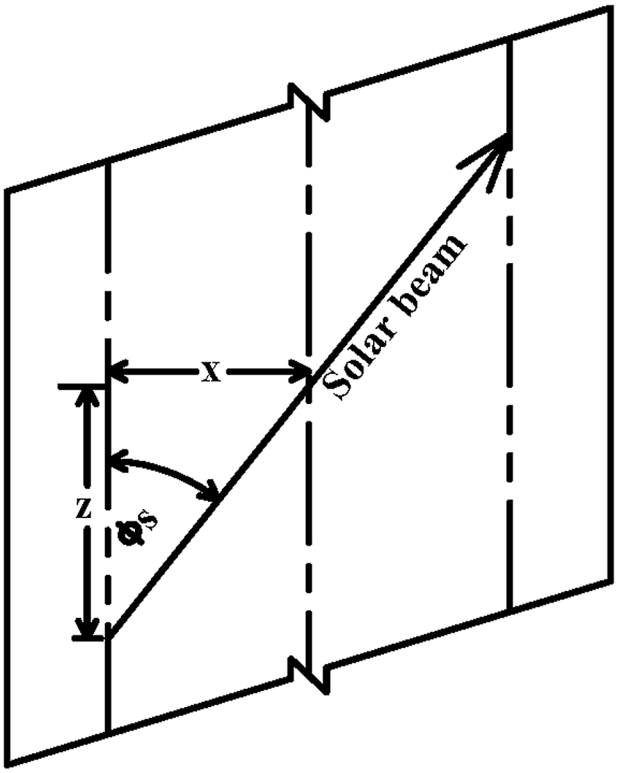

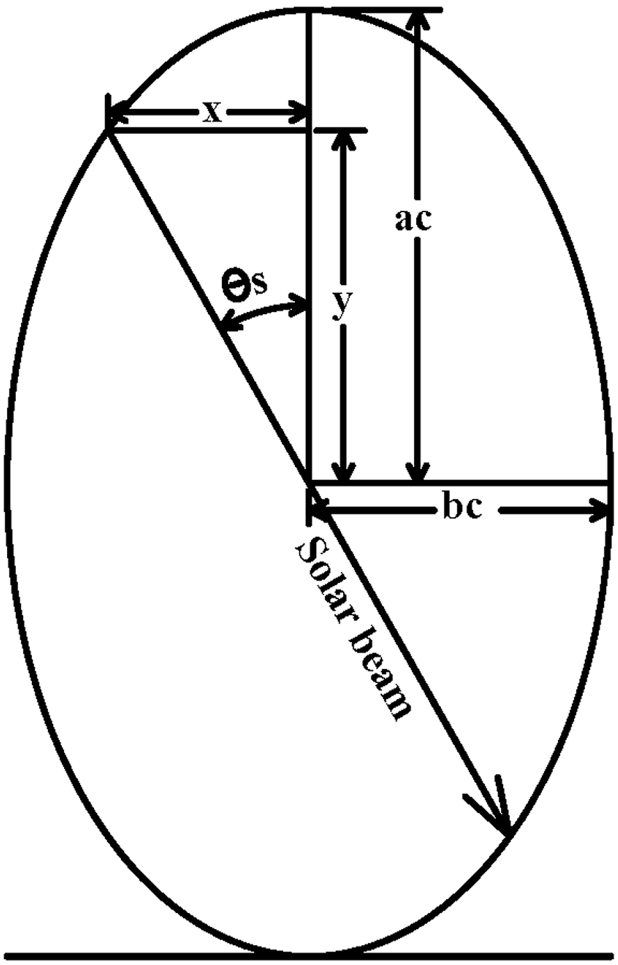

Fig. A4. Parameters used to calculate the path length fraction of a solar beam through a canopy modeled as an elliptical hedgerow.

$$N_R = \text{roundup}\left[\left(V_R/r_V\right)\tan\left(\theta_{MR}\right)\sin\left(\varphi_R\right)\right]+2 \quad [A14]$$

where θ_{MR} is the maximum θ_R where interrows are visible, with two additional rows added to ensure that N_R is not underestimated. The θ_{MR} variable is calculated in a similar manner as θ_{SPCR}. In Eq. [A6], [A7], and [A10], if b_C is substituted with $b_C/\sin(\Phi_R)$, r_V substituted with $r_V/\sin(\Phi_R)$, and θ_{SP} and θ_{SPCR} are substituted with θ_{MR}, it can be shown that

$$\tan\left(\theta_{MR}\right) = \frac{r_V\sqrt{1-4b_C^2/r_V^2}}{2a_C\sin\left(\varphi_R\right)} \quad [A15]$$

The computation of f_{DHC} pertains to the canopy, which is considered to be a composite of soil and vegetation because the canopy is considered to be porous. Therefore, a significant amount of substrate (soil) may be visible beneath the canopy under certain conditions, such as for vertical (prolate) leaf inclination or small canopies. If this is not accounted for in the transmittance and reflectance terms, then f_{DHC} must be reduced to include only vegetation. The downward hemispherical vegetation view factor (f_{DHV}) is then defined as

$$f_{DHV} = f_{DHC} - f_{DHSE} \quad [A16]$$

where f_{DHSE} is the downward hemispherical view factor of soil visible beneath the canopy by extinction, calculated as

$$f_{DHSE} = \frac{2}{\pi^2}\int_0^{\pi/2}\left\{\sum_{i=-N_R(\varphi_R)}^{i=+N_R(\varphi_R)}\max\left[0,\left(\theta_{R(2,i)}-\theta_{R(1,i)}\right)\tau_C\right]\right\}d\varphi_R \quad [A17]$$

where τ_C can be calculated to account for either shortwave (e.g., Eq. [2]) or longwave extinction through the canopy. Canopy rows (and not soil appearing in the interrows) are of primary interest in calculating f_{DHSE}. Therefore, N_R should be calculated for nearly the entire hemispherical view in Eq. [A17], where θ_{MR} and Φ_R are replaced with ~85 and 90°, respectively, in Eq. [A14].

The upward-line-integrated hemispherical canopy view factor (f_{UIC}) applies to diffuse irradiance that is transmitted to the soil surface in TR_S and TPAR, which are measured by line radiometers. It is calculated by integrating f_{DHC} from the center of the crop row to the center of the interrow, i.e., $0 \le P_R \le r_V/2$, and setting $V_R = h_C$:

$$f_{UIC} = \int_0^{r_V/2} f_{DHC}\left(V_R = h_C\right)dP_R \quad [A18]$$

APPENDIX 4

Path Length Fraction and Multiple Row Factor Used in the Elliptical Hedgerow Model

The path length fraction (P_L) and multiple row factor (M_R) terms used in Eq. [7] were derived as part of the elliptical hedgerow model; P_L and M_R account for the nonrandom distribution of vegetation in row crops for a shortwave solar beam propagating through a canopy. The P_L is the length fraction relative to vertical for a beam through a canopy. For uniform canopies, $P_L = h_C/\cos(\theta_S)$, where h_C is the canopy height and θ_S is the solar zenith angle, but for row crops, P_L also depends on the solar azimuth relative to the crop row (Φ_S) and the canopy width (w_C). Then P_L is defined as (Fig. A4)

$$P_L \equiv \frac{\sqrt{x^2+y^2+z^2}}{a_C} \quad [A19]$$

where

$$y = \frac{a_C b_C}{\sqrt{a_C^2\tan^2\left(\theta_{SP}\right)+b_C^2}} \quad [A20]$$

$$x = y\tan\left(\theta_{SP}\right) \quad [A21]$$

$$z = \frac{x}{\tan\left(\Phi_S\right)} \quad [A22]$$

and θ_{SP} is calculated by Eq. [A4].

For large θ_S or h_C greater than the crop row spacing (r_V), a solar beam will probably traverse multiple rows, which is accounted for by M_R. Consider three crop rows (modeled as elliptical hedgerows) with row spacing r_V and major and minor semiaxes a_C and b_C, respectively (Fig. A5). Beginning with the row on the left, there are $n = 1$ and $n = 2$ adjacent rows to the right, each with a corresponding tangent. Each tangent contacts the far left ellipse a distance $X_{SCR}(n)$ from its center, derived from Eq. [A11] but now having n multiple rows:

$$X_{SCR}(n) = \frac{2b_C^2}{nr_V} \quad [A23]$$

A solar beam tangent to the far left ellipse a distance X_S from its center (see Eq. [A8]), where $X_{SCR}(2) \le X_S \le X_{SCR}(1)$, will pass through row $n = 1$. In general, a beam will pass through row n where $X_{SCR}(n+1) \le X_S \le X_{SCR}(n)$. Then M_R is defined as

$$M_R \equiv \begin{cases} n+\dfrac{X_{SCR}(n)-X_S}{X_{SCR}(n)-X_{SCR}(n+1)} \\ \qquad \text{for } X_{SCR}(n+1) \le X_S \le X_{SCR}(n) \\ 1.0 \qquad\qquad \text{for } X_S \ge X_{SCR}(1) \end{cases} \quad [A24]$$

Beginning with $n = 1$, n is incremented by 1 until $X_S > X_{SCR}(n)$.

ACKNOWLEDGMENTS

This research was supported by the USDA-ARS National Program 211, Water Availability and Watershed Management and by the USDA-ARS Ogallala Aquifer Program, a consortium between USDA-ARS, Kansas State University, Texas AgriLife Research, Texas AgriLife Extension Service, Texas Tech University, and West Texas A&M University. We are grateful to the numerous biological technicians and student workers for their meticulous and dedicated efforts in executing experiments and obtaining and processing data.

REFERENCES

Allen, R.G., L.S. Pereira, D. Raes, and M. Smith. 1998. Crop evapotranspiration: Guidelines for computing crop water requirements. Irrig. Drain. Pap. 56. FAO, Rome.

Anderson, M.C., J.M. Norman, W.P. Kustas, F. Li, J.H. Prueger, and J.R. Mecikalski. 2005. Effects of vegetation clumping on two-source model estimates of surface energy fluxes from an agricultural landscape during SMACEX. J. Hydrometeorol. 6:892–909. doi:10.1175/JHM465.1

Annandale, J.G., N.Z. Jovanovic, G.S. Campbell, N. Du Sautoy, and P. Lobit. 2004. Two-dimensional solar radiation interception model for hedgerow fruit trees. Agric. For. Meteorol. 121:207–225. doi:10.1016/j.agrformet.2003.08.004

Arkin, G.F., J.T. Richie, and S.J. Maas. 1978. A model for calculating light interception by a grain sorghum canopy. Trans. ASAE 21:303–308.

Campbell, G.S. 1986. Extinction coefficients for radiation in plant canopies calculated using an ellipsoidal inclination angle distribution. Agric. For. Meteorol. 36:317–321. doi:10.1016/0168-1923(86)90010-9

Campbell, G.S. 1990. Derivation of an angle density function for canopies with ellipsoidal leaf angle distributions. Agric. For. Meteorol. 49:173–176. doi:10.1016/0168-1923(90)90030-A

Campbell, G.S., and J.M. Norman. 1998. An introduction to environmental biophysics. 2nd ed. Springer-Verlag, New York.

Charles-Edwards, D.A., and J.H.M. Thornley. 1973. Light interception by an isolated plat: A simple model. Ann. Bot. 37:919–928.

Charles-Edwards, D.A., and M.R. Thorpe. 1976. Interception of diffuse and direct-beam radiation by a hedgerow apple orchard. Ann. Bot. 40:603–613.

Chen, J. 1984. Mathematical analysis and simulation of crop micrometeorology. Ph.D. diss. Wageningen Agricultural Univ., Wageningen, the Netherlands.

Chen, J.M. 1996. Optically-based methods for measuring seasonal variation of leaf area index in boreal conifer stands. Agric. For. Meteorol. 80:135–163. doi:10.1016/0168-1923(95)02291-0

Clark, D.H., D.A. Johnson, K.D. Kephart, and N.A. Jackson. 1995. Near infrared reflectance spectroscopy estimation of ^{13}C discrimination in forages. J. Range Manage. 48:132–136. doi:10.2307/4002799

Colaizzi, P.D., R.C. Schwartz, S.R. Evett, T.A. Howell, P.H. Gowda, and J.A. Tolk. 2012. Radiation model for row crops: 2. Model evaluation. Agron. J. 104:XXX–XXX (this issue).

Doraiswamy, P.C., J.L. Hatfield, T.J. Jackson, B. Akhmedov, J. Prueger, and A. Stern. 2004. Crop condition and yield simulations using Landsat and MODIS. Remote Sens. Environ. 92:548–559. doi:10.1016/j.rse.2004.05.017

Evett, S.R., T.A. Howell, and A.D. Schneider. 1995. Energy and water balances for surface and subsurface drip irrigated corn. p. 135–140. *In* F.R. Lamm (ed.) Microirrigation for a changing World: Conserving resources/preserving the environment, Proc. Int. Microirrigation Congr., 5th, Orlando, FL. 2–6 Apr. 1995. ASABE, St. Joseph, MI.

Evett, S.R., and R.J. Lascano. 1993. ENWATBAL.BAS: A mechanistic evapotranspiration model written in compiled Basic. Agron. J. 85:763–772. doi:10.2134/agronj1993.00021962008500030044x

Flerchinger, G.N., W. Xiao, T.J. Sauer, and Q. Yu. 2009. Simulation of within-canopy radiation exchange. NJAS Wageningen J. Life Sci. 57:5–15. doi:10.1016/j.njas.2009.07.004

French, A.N., D.J. Hunsaker, T.R. Clarke, G.J. Fitzgerald, W.E. Luckett, and P.J. Pinter, Jr. 2007. Energy balance estimation of evapotranspiration for wheat grown under variable management practices in central Arizona. Trans. ASABE 50:2059–2071.

Gausman, H.W., and W.A. Allen. 1973. Optical parameters of leaves of 30 plant species. Plant Physiol. 52:57–62. doi:10.1104/pp.52.1.57

Goudriaan, J. 1977. Crop micrometeorology: A simulation study. Pudoc, Wageningen, the Netherlands.

Goudriaan, J. 1988. The bare bones of leaf-angle distribution in radiation models for canopy photosynthesis and energy exchange. Agric. For. Meteorol. 43:155–169. doi:10.1016/0168-1923(88)90089-5

Graser, E.A., and C.H.M. van Bavel. 1982. The effect of soil moisture upon soil albedo. Agric. Meteorol. 27:17–26. doi:10.1016/0002-1571(82)90015-2

Ham, J.M., and G.J. Kluitenberg. 1993. Positional variation in the soil energy balance beneath a row-crop canopy. Agric. For. Meteorol. 63:73–92. doi:10.1016/0168-1923(93)90023-B

Howell, T.A., S.R. Evett, J.A. Tolk, and A.D. Schneider. 2004. Evapotranspiration of full-, deficit-irrigated, and dryland cotton on the northern Texas High Plains. J. Irrig. Drain. Eng. 130:277–285. doi:10.1061/(ASCE)0733-9437(2004)130:4(277)

Howell, T.A., J.L. Steiner, S.R. Evett, A.D. Schneider, K.S. Copeland, D.A. Dusek, and A. Tunick. 1993. Radiation balance and soil water evaporation of bare Pullman clay loam soil. p. 922–929. *In* R.G. Allen and C.M.U. Neale (ed.) Management of irrigation and drainage systems: Integrated perspectives. Am. Soc. Civ. Eng., New York.

Howell, T.A., J.L. Steiner, A.D. Schneider, S.R. Evett, and J.A. Tolk. 1997. Seasonal and maximum daily evapotranspiration of irrigated winter wheat, sorghum, and corn: Southern High Plains. Trans. ASAE 40:623–634.

Idso, S.B., R.J. Reginato, R.D. Jackson, B.A. Kimball, and F.S. Nakayama. 1974. The three stages of drying of a field soil. Soil Sci. Soc. Am. J. 38:831–837. doi:10.2136/sssaj1974.03615995003800050037x

Jacovides, C.P., F.S. Tymvios, V.D. Assimakopulos, and N.A. Kaltsounides. 2007. The dependence of global and diffuse PAR radiation components on sky conditions at Athens, Greece. Agric. For. Meteorol. 143:277–287. doi:10.1016/j.agrformet.2007.01.004

Kucharik, C.J., J.M. Norman, and S.T. Gower. 1999. Characterization of radiation regimes in nonrandom forest canopies: Theory, measurements, and a simplified modeling approach. Tree Physiol. 19:695–706.

Kustas, W.P., and J.M. Norman. 1999. Evaluation of soil and vegetation heat flux predictions using a simple two-source model with radiometric temperatures for partial canopy cover. Agric. For. Meteorol. 94:13–29. doi:10.1016/S0168-1923(99)00005-2

Lascano, R.J., C.H.M. van Bavel, J.L. Hatfield, and D.R. Upchurch. 1987. Energy and water balance of a sparse crop: Simulated and measured soil and crop evaporation. Soil Sci. Soc. Am. J. 51:1113–1121. doi:10.2136/sssaj1987.03615995005100050004x

Lasdon, L.S., A.D. Waren, A. Jain, and M. Ratner. 1978. Design and testing of a generalized reduced gradient code for nonlinear programming. ACM Trans. Math. Softw. 4:34–50. doi:10.1145/355769.355773

Legates, D.R., and G.J. McCabe, Jr. 1999. Evaluating the use of "goodness-of-fit" measures in hydrologic and hydroclimatic model validation. Water Resour. Res. 35:233–241. doi:10.1029/1998WR900018

Li, F., W.P. Kustas, J.H. Prueger, C.M.U. Neale, and T.J. Jackson. 2005. Utility of remote sensing-based two-source energy balance model under low- and high-vegetation cover conditions. J. Hydrometeorol. 6:878–891. doi:10.1175/JHM464.1

López, G., T. Muneer, and R. Claywell. 2004. Comparative study of four shadow band diffuse irradiance correction algorithms for Almería, Spain. J. Sol. Energy Eng. 126:696–701. doi:10.1115/1.1666895

Mann, J.E., G.L. Curry, D.W. DeMichele, and D.N. Baker. 1980. Light penetration in a row-crop with random plant spacing. Agron. J. 72:131–142. doi:10.2134/agronj1980.00021962007200010026x

McCree, K.J. 1972. Test of current definitions of photosynthetically active radiation against leaf photosynthesis data. Agric. Meteorol. 10:443–453. doi:10.1016/0002-1571(72)90045-3

Meek, D.W., J.L. Hatfield, T.A. Howell, S.B. Idso, and R.J. Reginato. 1984. A generalized relationship between photosynthetically active radiation and solar radiation. Agron. J. 76:939–945. doi:10.2134/agronj1984.00021962007600060018x

Moriasi, D.N., J.G. Arnold, M.W. Van Liew, R.L. Bingner, and T.L. Veith. 2007. Model evaluation guidelines for systematic quantification of accuracy in watershed simulations. Trans. ASABE 50:885–900.

Muneer, T., and X. Zhang. 2002. A new method for correcting shadow band diffuse irradiance data. J. Sol. Energy Eng. 124:34–43. doi:10.1115/1.1435647

Nash, J.E., and J.V. Sutcliffe. 1970. River flow forecasting through conceptual models: 1. A discussion of principles. J. Hydrol. 10:282–290. doi:10.1016/0022-1694(70)90255-6

Nilson, T. 1971. A theoretical analysis of the frequency of gaps in plant stands. Agric. Meteorol. 8:25–38. doi:10.1016/0002-1571(71)90092-6

Norman, J.M., and J.M. Welles. 1983. Radiative transfer in an array of canopies. Agron. J. 75:481–488. doi:10.2134/agronj1983.00021962007500030016x

NRCS. 2011. Web soil survey: Soil survey TX375, Potter County, Texas. Available at websoilsurvey.nrcs.usda.gov (accessed 8 Aug. 2011; verified 10 Dec. 2011). NRCS, Washington, DC.

Oyarzun, R.A., C.O. Stöckle, and M.D. Whiting. 2007. A simple approach to modeling radiation interception by fruit-tree orchards. Agric. Meteorol. 142:12–24. doi:10.1016/j.agrformet.2006.10.004

Pieri, P. 2010a. Modelling radiative balance in a row-crop canopy: Row–soil surface net radiation partition. Ecol. Modell. 221:791–801. doi:10.1016/j.ecolmodel.2009.11.019

Pieri, P. 2010b. Modeling radiative balance in a row-crop canopy: Cross-row distribution of net radiation at the soil surface and energy available to clusters in a vineyard. Ecol. Modell. 221:802–811. doi:10.1016/j.ecolmodel.2009.07.028

Servat, E., and A. Dezetter. 1991. Selection of calibration objective functions in the context of rainfall–runoff modeling in a Sudanese savannah area. Hydrol. Sci. J. 36:307–330. doi:10.1080/02626669109492517

Steiner, J.L., T.A. Howell, and A.D. Schneider. 1991. Lysimetric evaluation of daily potential evapotranspiration models for grain sorghum. Agron. J. 83:240–247. doi:10.2134/agronj1991.00021962008300010055x

Task Committee on Standardization of Reference Evapotranspiration. 2005. The ASCE standardized reference evapotranspiration equation. Available at www.kimberly.uidaho.edu/water/asceewri/ascestzdetmain2005.pdf (accessed 6 July 2011; verified 10 Dec. 2011). ASCE Environ. Water Resour. Inst., Reston, VA.

Thanisawanyangkura, S., H. Sinoquet, P. Rivet, M. Cretenet, and E. Jallas. 1997. Leaf orientation and sunlit leaf area distribution in cotton. Agric. For. Meteorol. 86:1–15. doi:10.1016/S0168-1923(96)02417-3

Tolk, J.A., T.A. Howell, J.L. Steiner, and D.R. Krieg. 1995. Aerodynamic characteristics of corn as determined by energy balance techniques. Agron. J. 87:464–473. doi:10.2134/agronj1995.00021962008700030012x

Tunick, A., H. Rachele, F.V. Hansen, T.A. Howell, J.L. Steiner, A.D. Schneider, and S.R. Evett. 1994. REBAL '92: A cooperative radiation and energy balance field study for imagery and electromagnetic propagation. Bull. Am. Meteorol. Soc. 75:421–430. doi:10.1175/1520-0477(1994)0752.0.CO;2

Weiss, A., and J.M. Norman. 1985. Partitioning solar radiation into direct an diffuse, visible and near-infrared components. Agric. For. Meteorol. 34:205–213.

Williams, L.E., and J.E. Ayars. 2005. Grapevine water use and the crop coefficient are linear functions of the shaded area measured beneath the canopy. Agric. For. Meteorol. 132:201–211. doi:10.1016/j.agrformet.2005.07.010

Xiao, W., G.N. Flerchinger, Q. Yu, and Y.F. Zheng. 2006. Evaluation of the SHAW model in simulating the components of net all-wave radiation. Trans. ASABE 49:1351–1360.

Yeh, W.W.-G. 1986. Review of parameter identification procedures in groundwater hydrology: The inverse problem. Water Resour. Res. 22:95–108. doi:10.1029/WR022i002p00095

Zhao, W., and R.J. Qualls. 2005. A multiple-layer canopy scattering model to simulate shortwave radiation distribution within a homogenous plant canopy. Water Resour. Res. 41:W08409. doi:10.1029/2005WR004016